OXFORD

Cerebral Cortex, October 2019; 4169–4193

doi: 10.1093/cercor/bhy300
Advance Access Publication Date: 11 October 2018
Original Article

ORIGINAL ARTICLE

Age-Related Differences in Brain Morphology and the Modifiers in Middle-Aged and Older Adults

Lu Zhao[1], William Matloff[1], Kaida Ning[1], Hosung Kim[1], Ivo D. Dinov[2,3] and Arthur W. Toga[1]

[1]Laboratory of Neuro Imaging, USC Mark and Mary Stevens Neuroimaging and Informatics Institute, University of Southern California, Los Angeles, CA 90033, USA, [2]Statistics Online Computational Resource, HBBS, University of Michigan, Ann Arbor, MI 48109-2003, USA and [3]Michigan Institute for Data Science, HBBS, University of Michigan, Ann Arbor, MI 48109-1042, USA

Address correspondence to Arthur W. Toga, USC Stevens Neuroimaging and Informatics Institute, Keck School of Medicine of USC, University of Southern California, 2025 Zonal Ave., Los Angeles, CA 90033, USA. Email: toga@loni.usc.edu

Abstract

Brain structural morphology differs with age. This study examined age-differences in surface-based morphometric measures of cortical thickness, volume, and surface area in a well-defined sample of 8137 generally healthy UK Biobank participants aged 45–79 years. We illustrate that the complexity of age-related brain morphological differences may be related to the laminar organization and regional evolutionary history of the cortex, and age of about 60 is a break point for increasing negative associations between age and brain morphology in Alzheimer's disease (AD)-prone areas. We also report novel relationships of age-related cortical differences with individual factors of sex, cognitive functions of fluid intelligence, reaction time and prospective memory, cigarette smoking, alcohol consumption, sleep disruption, genetic markers of apolipoprotein E, brain-derived neurotrophic factor, catechol-O-methyltransferase, and several genome-wide association study loci for AD and further reveal joint effects of cognitive functions, lifestyle behaviors, and education on age-related cortical differences. These findings provide one of the most extensive characterizations of age associations with major brain morphological measures and improve our understanding of normal structural brain aging and its potential modifiers.

Key words: aging, brain morphology, magnetic resonance imaging, modifiers of brain aging, surface-based morphometry

Introduction

Extant literature has demonstrated that the brain deteriorates with age both in basic and higher order cognitive functions (Reuter-Lorenz and Park 2010; Harada et al. 2013). Such age-induced cognitive declines are likely partly caused by macro-structural brain changes even in the absence of dementia or other pathological conditions (Kaup et al. 2011; Persson et al. 2012; Leong et al. 2017). Thus, an accurate characterization of how and where the brain macrostructure changes with age are important for understanding normal brain aging and would assist in identifying age-related neuropathology (Fjell and Walhovd 2010). Magnetic resonance imaging (MRI) has been widely applied to quantify the volume, thickness, and other morphometrics of specific brain structures in vivo, yielding anatomical insights into the human brain during aging.

Although it is clear that the brain atrophies with age and the related aging process are regionally heterochronic, existing findings are largely inconsistent in the characterization of the trajectory and spatial distribution of age effects across the brain (for a review, see (Fjell and Walhovd 2010; Kennedy and Raz 2015)). Previous MRI studies, with either a cross-sectional or longitudinal design, commonly use cohorts of participants with

a sample size being constrained by the expense and time of imaging acquisition (at most around 1000 participants (Crivello et al. 2014; Fjell et al. 2014)). Cohort effects and sampling bias that exist in the limited study samples prevent these studies from yielding true population-based findings; and a small sample size may not provide sufficient statistical power to detect subtle age effects. Moreover, much of the previous neuroanatomical measures were obtained using volumetric methods (Raz et al. 1997; 2005, 2010; Fjell et al. 2009; Ziegler et al. 2012; Crivello et al. 2014). Cortical volume (CVo) geometrically is a combination of cortical thickness (CTh) and cortical surface area (CSA), which are driven by distinct cellular mechanisms (Rakic 1988; Pontious et al. 2008) and differentially affected by genetic factors (Panizzon et al. 2009; Winkler et al. 2010). Some recent studies (Hogstrom et al. 2013; Zhao et al. 2013; Storsve et al. 2014; Dotson et al. 2015) also have shown that CTh and CSA were differentially affected by the aging process. Thus, studies using a single type of structural measure would be unable to provide a complete understanding of the mechanism underlying age-related brain structural differences or changes, as different measures may convey properties that are unique to others.

Additionally, complete understanding of the neurobiological, environmental, and genetic factors affecting the differential cortical declines remains unclear. The neuropil (axons, dendrites, and their collateral branches) accounts for the cortical gray matter (GM) volume and can expand and contract in response to multiple environmental changes (Kassem et al. 2013), and this may be crucial to the cortical atrophy observed in brain aging. Twin-studies have revealed the high heritability of brain structures (Toga and Thompson 2005; Peper et al. 2007; Chiang et al. 2009) and that the relationships of brain morphology with cognitive functions are substantially mediated by genetic factors (Posthuma et al. 2002; Thompson et al. 2002; Chiang et al. 2009). Identifying genetic influences on age-related structural differences or changes will provide a better understanding of the neurobiological mechanisms involved in aging. These limitations in existing imaging studies suggest that a statistically well-powered, system-level study is needed to characterize the differential age trajectories of diverse brain morphological measures and to investigate the impacts of various potential environmental and genetic modifiers on the identified aging effects.

In this study, we assessed the age-related differences in MRI-derived measures of CTh, CVo, and CSA across the cortex in a large community-based sample of 8137 healthy middle-aged to older adults from the UK Biobank resource (http://www.ukbiobank.ac.uk). All MRI scans were collected on a maximally homogeneous imaging platform and protocol (Miller et al. 2016; Alfaro-Almagro et al. 2017). A surface-based morphometry (SBM) framework (Salat et al. 2004) was utilized to detect brain morphology–age associations and estimate the mean cross-sectional trajectories at each cortical vertex. In contrast to voxel-based approaches (Ziegler et al. 2012; Crivello et al. 2014), SBM allows direct modeling of diverse morphological characteristics of the cortex. The vertex-wise analyses are able to detect even very small regions that exhibit age-related differences, which might be neglected in region of interest (ROI)-based methods (Raz et al. 2010; Lemaitre et al. 2012). Next, we analyzed the associations of cognitive functions (fluid intelligence, reaction time, visual memory, and prospective memory), lifestyle behaviors (cigarette smoking, alcohol consumption, and sleep), sex, education as well as specific genetic factors with age-related brain morphological differences. The target genetic factors included the apolipoprotein E (APOE), brain-derived neurotrophic factor (BDNF), catechol-O-methyltransferase (COMT), KOLTHO, and the top 21 Alzheimer's disease (AD)-risk/preventive genes (Lambert et al. 2013) (in addition to APOE). These genetic variants were selected because they have been the most frequently linked to variations in age-sensitive cognitive functions and/or neurodegeneration (Raz et al. 2009; Lambert et al. 2013; Dubal et al. 2014; 2015; Stage et al. 2016), however, their influences on age-related cortical differences or changes are still unclear. Moreover, cognitive functions and environmental factors are often interrelated in old adults (Hagger-Johnson et al. 2013; Kyle et al. 2017; Piumatti et al. 2018). Therefore, we further analyzed principal component analysis (PCA)-derived combinations of the cognitive and lifestyle factors as well as education in order to determine if there exist joint effects of these potential modifiers on age-related brain morphological differences. This study provides the best powered and the most comprehensive characterization to date of age-related brain structural differences and potential modifiers in middle to older ages.

Materials and Methods

Participants

The UK Biobank enrolled about 500 000 community-dwelling participants from across the United Kingdom, aged 40–69 years at baseline recruitment, from 2006 to 2010 (http://www.ukbiobank.ac.uk). Extensive health and lifestyle questionnaires, physical and cognitive measures, biological samples, and genotyping data were collected. In 2014, the UK Biobank started an imaging extension, aiming to collect head, heart, and body imaging from 100 000 participants in the existing cohort. We used brain MRI imaging data (UK Biobank data-field: 110) from the recent release (Feb 2017) of 10 102 participants (http://biobank.ctsu.ox.ac.uk/crystal/label.cgi?id=110). Ethical approval was obtained from the research ethics committee (REC reference 11/NW/0382). The present analyses were conducted under UK Biobank application number 25 641. All participants provided informed consent to participate. Further information on the consent procedure can be found at http://biobank.ctsu.ox.ac.uk/crystal/field.cgi?id=200. This study discarded 169 participants whose raw MRI scans did not pass manual quality assessment and other 19 participants due to failed image processing. A total of 422 participants who reported a diagnosis of neurological or psychiatric disorder at scanning (UK Biobank data-field: 20 002) were excluded as well (excluded disorders are listed in Supplementary Table S1). We further removed 1355 participants who did not have white British ancestry and/or did not pass the sample quality control for the genetic data (https://biobank.ctsu.ox.ac.uk/crystal/label.cgi?id=100313).

Demographic, Cognitive, and Lifestyle Information

This study utilized the demographic, cognitive, and lifestyle information collected at the MRI assessment (2014+). Educational qualifications (UK Biobank data-field: 6138) consisted of 8 categories: college or university degree/A levels or AS levels or equivalent/CSEs or equivalent/O levels or GCSEs or equivalent/NVQ or HND or HNC or equivalent/other professional qualifications, for example, nursing, teaching/none of the above/prefer not to answer. We collapsed the data into a binary variable indicating if a participant held a college or university degree so as to characterize the participants here. The self-reported sex (UK Biobank data-field: 31) was compared against genetic sex (UK Biobank

data-field: 22 001) to identify individuals with discordant sex information.

The cognitive tests included fluid intelligence (UK Biobank data-field: 100 027), reaction time (UK Biobank data-field: 100 032), visual memory (UK Biobank data-field: 100 030), and prospective memory (UK Biobank data-field: 100 031), all of which were administered via computerized touch screen interface. The fluid intelligence task assessed the ability to solve 13 verbal and numeric reasoning problems. Each problem had five possible response options. The dependent variable was the total number of correct answers given (range 0–13) within a 2-min period, with higher scores indicating better performance. The reaction time task was delivered in the style of the card game, "snap," and requested participants to respond with a button press when they detected the appearance of a matching pair of symbols. The dependent variable was the mean response time in milliseconds across 12 matching-pair trials. In the visual memory task, 6 card pairs of symbols were presented on-screen in a random pattern. Cards were then turned face down on the screen, and participants were asked to locate as many symbol pairs as possible in as few attempts as possible. The dependent variable was the number of errors made during pairs matching (range 0–146), which was log-transformed because of skewed distribution and zero inflation [ln (x + 1)]. In the prospective memory task, participants were asked to remember to perform a preplanned instruction. Participants were categorized depending on whether they completed the task on first attempt or not. More details about the UK Biobank cognitive tests are available in the study by Lyall et al. (2016).

The lifestyle behaviors we focused in this work were tobacco smoking, alcohol consumption, and sleep. Information on current and past smoking characteristics, including age at smoking initiation (UK Biobank data-field: 3436 and 2867), number of cigarettes smoked per day (UK Biobank data-field: 3456 and 2887), age when stopped smoking (ex-smokers only) (UK Biobank data-field: 6194), was assessed using the touch screen questionnaire. The smoking status of participants was classified as: current smokers, ex-smokers or lifetime nonsmokers (UK Biobank data-field: 20 116). Duration of smoking was calculated from the age the participant started smoking and the date of MRI assessment (or, among ex-smokers, the age when they stopped smoking). The number of pack-years for ex-smokers and current smokers was calculated by multiplying the number of cigarettes smoked per day by the years of smoking and divided by 20.

Alcohol consumption was measured using the question "about how often do you drink alcohol?" Available responses were "daily or almost daily," "three of four times a week", "once or twice a week," "one to three times a month", "special occasions only," "never," and "prefer not to answer" (UK Biobank Data-Field 1558). Respondents who drank alcohol once a week or more frequently were asked to record how many alcoholic drinks they consumed on average each week from a list of common alcoholic beverages (red and white wine, champagne, beer and cider, spirits and liquors, fortified wine, and other alcoholic drinks), or to respond "do not know" or "prefer not to answer" (UK Biobank Data-Fields 1568, 1678, 1588, 1598, 1608, and 5364). Volumes were specified when referring to beverages (e.g., "there are six glasses in an average bottle of wine"; "there are 25 standard measures in a normal sized bottle"). Respondents who declared that they drank alcohol "one to three times a month" or on "special occasions only" (henceforth monthly drinkers) were also asked to record how many drinks they consumed on average each month (UK Biobank data-fields 4407, 4418, 4429, 4440, 4451, 4462). Alcohol consumption in grams per day was calculated by multiplying the average number of alcoholic drinks consumed each week/month by the average grams of alcohol contained in each type of drink, determined using the UK Food Standard Agency's guidelines (Roe et al. 2015). The total was then divided by 7 (or 30 for monthly drinkers) to provide mean daily alcohol consumption. Alcohol consumption was positively skew and log-transformed. The number of drink units consumed per day/week were calculated from the daily alcohol consumptions in grams (one drink unit contains ~8 g of pure alcohol in UK). Because of the possible U-shaped relationship between alcohol consumption and the neurological outcomes (Ruitenberg et al. 2002; Mukamal et al. 2003; Luchsinger et al. 2004; Stampfer et al. 2005), participants were classified into groups of abstainers (<1 unit/week), 1–<7 units/week, 7–<14 units/week, 14– <21 units/week, 21–<30 units/week, and >30 units/week as suggested in recent studies (Topiwala et al. 2017).

Insomnia symptoms were assessed using the question "Do you have trouble falling asleep at night or do you wake up in the middle of the night?" Available responses were "never/rarely," "sometimes," and "usually" (UK Biobank Data-Fields 1200). Participants were categorized as having frequent insomnia symptoms if they answered "usually" to this question, while the remaining participants made up the control group without frequent insomnia symptoms. Sleep duration was recorded as the number of reported hours to the following question: "About how many hours sleep do you get in every 24 hours (include naps)" (UK Biobank Data-Fields 1160). Given previously established U-shape relationships with health and cognition (Lo et al. 2016), we categorized sleep duration into short (<7 h), normal (7–9 h), and long (>9 h) based on recent guidelines (Watson et al. 2015).

Genetic Data and Processing

All UK Biobank participants were genotyped using the Affymetrix UK BiLEVE Axiom array (on an initial ~50 000 participants) and the Affymetrix UK Biobank Axiom array (on the remaining ~450 000 participants) were genotyped using the Affymetrix UK Biobank Axiom array. The two single-nucleotide polymorphism (SNP) arrays are very similar with over 95% common marker content. In total, about 800 000 markers were genotyped for each participant. The UK Biobank team first imputed the genotyping data using the Haplotype Reference Consortium (HRC) reference panel and then imputed the SNPs not in the HRC panel using a combined UK10K + 1000 Genomes panel. The imputation process produced a dataset with >92 million autosomal SNPs. Detailed information and documentation on the genotyping, imputation, and QC are available at http://www.ukbiobank.ac.uk/scientists-3/genetic-data/. We excluded the subjects who were identified to have discordant sex information or were outliers in heterozygosity and missing rates, or had a relatedness corresponding to third-degree relatives or closer, or do not have a white British ancestry. The target SNPs were extracted from the imputed arrays, which all had an imputation information score >0.96. APOE ε4 allele status was determined by combining allelic results from the APOE SNPS rs429358 and rs7412. The combination of these 2 SNPs result in cysteine-to-arginine amino acid substitutions in APOE at positions 130 and 176. The E2 allele is represented by the Cys–Cys combination, ε3 by the Cys130–Arg176 combination, and ε4 by the Arg–Arg combination (Ghebranious et al. 2005). The haplotype KL-VS that increases klotho secretion (Dubal et al. 2014) were defined by segregating 2 variants in the *KLOTHO* gene,

Table 1 Sample characteristics

Variable	M (SD), min–max if applicable	N
Demographics		
Age at MRI in years	62.69 (7.44), 45.17–79.37	8137
Gender, male (%)	3882 (47.71%)	8137
Obtained college degree, yes (%)	3629 (45.02%)	8061
Ethnicity, white British ancestry (%)	8137 (100%)	8137
Cognitive tests		
Fluid intelligence score	6.96 (2.09), 1–13	7775
Prospective memory, successful N (%)	7311 (90.59%)	8070
Raw reaction time in milliseconds, median (IQR)	566 (125), 351–1684	8046
Log-transformed reaction time	6.36 (0.17), 5.86–7.42	8046
Raw visual memory errors, median (IQR)	3 (4), 0–27	8084
Log-transformed visual memory errors	1.29 (0.64), 0–3.33	8084
Life behaviors		
Smoking status, current/previous/never	320/2802/4942	8064
Pack-years of smoking	19.01 (14.71), 0.25–132.5	2005
Alcohol drinking status, weekly/monthly/nondrinkers	5898/1402/199	7499
Raw daily alcohol intake in grams, median (IQR)	12.46 (18.98), 0–161.18	7499
Log-transformed daily alcohol intake	2.45 (1.06), 0–5.088	7499
Alcohol consumption levels, <1/1-<7/7-<14/14-<21/21-<30/ >30 units/week	604/2041/1789/1181/ 841/1043	7499
Sleep duration in hours	7.17 (1.04), 2–15	8070
Sleep duration levels, >7/7–9/ >9 h	1883/6087/100	8070
Insomnia symptoms, frequent/infrequent	2405/5673	8078
APOE		
APOE genotype frequencies, N (%)	ε2/ε2: 48 (0.59%), ε2/ε3: 1006 (12.36%), ε2/ε4: 192 (2.36%), ε3/ε3: 4810 (59.11%), ε3/ε4: 1896 (23.30%), ε4/ε4: 185 (2.27%)	8137
KLOTHO		
KL-VS genotype frequencies, N (%)	noncarriers: 5733 (70.46%), heterozygotes: 2193 (27%), homozygotes: 207 (2.54%)	8137

Note: M = mean; SD = standard deviation; min = minimum; max = maximum; IQR = interquartile range.

rs9536314 (F352V) and rs9527025 (C370S), which were in perfect linkage disequilibrium in all samples genotyped (Pearson's $r = 1$).

MRI Acquisition and Processing

Details of the MRI acquisition is described in the UK Biobank Brain Imaging Documentation (http://biobank.ctsu.ox.ac.uk/crystal/refer.cgi?id=1977) and in a protocol form (http://biobank.ctsu.ox.ac.uk/crystal/refer.cgi?id=2367). Briefly, all participants were scanned using a single standard Siemens Skyra 3 T scanner with a standard Siemens 32-channel RF receive head coil. The T1-weighted structural MRI volumes were acquired using a 3D magnetization-prepared rapid gradient-echo (MPRAGE) sequence, with 1 mm isotropic resolution, a field-of-view (FOV) of 208 mm, and a 256 × 256 matrix. All released brain MRI images were defaced to protect study participant anonymity. Careful manual quality assessment was conducted for the whole imaging dataset by the UK Biobank team to identify images that were corrupted, missing, or otherwise unusable (Alfaro-Almagro et al. 2017).

All MR images were processed for reconstructing cortical surfaces and extracting morphological phenotypes using the FreeSurfer (v6.0) software package (http://surfer.nmr.mgh.harvard.edu/). The FreeSurfer processing was implemented on the LONI pipeline system for high-performance parallel computing (http://pipeline.loni.usc.edu). To obtain a comprehensive description for age-related differences in brain morphology, this work included 3 vertex-wise imaging measures acquired based on a cortical surface model (each hemispheric surface was consisted of 163 842 vertices) (Fischl and Dale 2000): CTh, CVo, and CSA. Prior to statistical analysis, the surface-based data were smoothed on the tessellated surfaces using a Gaussian kernel with the full-width half-maximum of 20 mm to increase the signal-to-noise ratio and to reduce the impact of misregistration. More information about the FreeSurfer processing and neuroimaging measures is given in the Supplementary Material.

Statistical Analyses

To determine the complex (linear and nonlinear) relationships between age and brain morphological measures, linear mixed-effects regression models were constructed at each cortical surface vertex with a step-down model selection procedure testing for cubic, quadratic, and linear age effects. Such method has been commonly used in previous studies of complex brain structural trajectories in neurodevelopment (Shaw et al. 2008) and aging (Terribilli et al. 2011; Pfefferbaum et al. 2013). The full model for the morphological measure (CTh, CVo, or CSA) T_i at a cortical point i is

$$T_i = \text{intercept} + \beta_1 \text{Age} + \beta_2 \text{Age}^2 + \beta_3 \text{Age}^3 + e_i,$$

where e is the residual error, and the intercept and β terms are the fixed effects. If the cubic age effect was not significant, the cubic term was removed and we stepped down to the quadratic

Table 2 Summary of SNPs of the studied genetic factors

SNP	Chromosome	Gene	Major/minor alleles	MAF	Imputation Info Score	
rs429358	19	APOE	T/C	0.154	1	
rs7412	19	APOE	C/T	0.080	1	
Val158Met (rs4680)	22	COMT	G(Val)/A(Met)	0.492	1	
Val66Met (rs6265)	11	BDNF	G(Val)/A(Met)	0.187	1	
F352V (rs9536314)	13	KLOTHO	T/G	0.160	1	
C370S (rs9527025)	13	KLOTHO	G/C	0.160	1	
GWAS-defined AD-associated loci						**PAF Type**
rs6656401	1	CR1	G/A	0.172	0.999	Risk
rs6733839	2	BIN1	C/T	0.391	0.963	Risk
rs35349669	2	INPP5D	C/T	0.483	0.997	Risk
rs190982	5	MEF2C	A/G	0.391	0.967	Preventive
rs10948363	6	CD2AP	A/G	0.271	0.999	Risk
rs9271192	6	HLA-DRB5–HLA-DRB1	A/C	0.274	0.999	Risk
rs11771145	7	EPHA1	G/A	0.351	1	Preventive
rs2718058	7	NME8	A/G	0.363	0.994	Preventive
rs1476679	7	ZCWPW1	T/C	0.302	0.997	Preventive
rs9331896	8	CLU	T/C	0.412	0.990	Preventive
rs28834970	8	PTK2B	T/C	0.365	0.996	Risk
rs983392	11	MS4A6A	A/G	0.401	0.994	Preventive
rs10792832	11	PICALM	G/A	0.366	0.999	Preventive
rs11218343	11	SORL1	T/C	0.040	0.992	Preventive
rs10838725	11	CELF1	T/C	0.300	0.999	Risk
rs10498633	14	SLC24A4-RIN3	G/T	0.227	1	Preventive
rs17125944	14	FERMT2	T/C	0.092	0.992	Risk
rs8093731	18	DSG2	C/T	0.020	1	Preventive
rs4147929	19	ABCA7	G/A	0.174	0.998	Risk
rs3865444	19	CD33	C/A	0.314	1	Preventive
rs7274581	20	CASS4	T/C	0.086	0.986	Preventive

model, and so on. The analyses were repeated controlling for sex and intracranial volume (ICV) as covariates. We further performed segmented regression analyses (Muggeo 2003; 2016) at the vertices that showed nonlinear age effects in order to statistically determine the existence of break points and their locations in the estimated mean cross-sectional age trajectories. Given a linear regression model, the segmented approach estimates a new model having broken-line relationships that are defined by the slope parameters and the break points where the linear relationship changes.

To examine the effects of potential modifiers on the age-related cortical differences, we repeated the linear mixed-effects regression analyses and assessed the interactions between age (or nonlinear age term) and cognitive functions, lifestyle behaviors, and genetic factors as well as sex and education. To assess potential joint effects of the behavioral and environmental factors, we conducted a PCA on the multivariate data of the cognitive, lifestyle variables, and education to extract new variables representing linear combinations of them. Instead of using the standard PCA that uses all the variables to produce each principal component (PC) regardless if a variable is a noise, we utilized a group-sparse block PCA method (Shen and Huang 2008; Journée et al. 2010; Chavent and Chavent 2017), which excludes ineffective variables from the PCA model with sparseness modeling. Additionally, prior to PCA, dummy coding was applied to categorical variables such as education, prospective memory test result, smoking status, alcohol drinker status, and insomnia status. The grouping strategy ensured that all dummy variables from the same categorical variable will be retained or excluded in the PCA model simultaneously. After PCA, the first 10 PCs that together explained over 95% of variance among the original multivariate data were selected, and the associations of these new variables with age-related brain structural differences were examined adjusting for age, sex, and ICV.

A false discovery rate (FDR) of $q < 0.05$ was applied to control for the multiple comparisons across all 327 684 brain surface vertices for each whole-brain test. A Bonferroni correction was further applied to adjust for the multiple whole-brain comparisons for linear/nonlinear age effects and different interactions on morphological measures, resulting in a critical threshold of $q < 0.05/291 = 1.72\text{E-}4$ (total number of whole-brain tests = 291). Results from the more lenient exploratory threshold $q < 0.05$ (but > 1.72E-4) were also reported here. The rationale for complementing the conservative $q < 1.72\text{E-}4$ results with results from this more lenient exploratory threshold is that further adjusting for the whole-brain tests might lead to false negatives, and the cost of a false negative could be missing out an important discovery (McDonald 2014). All the whole-brain analyses were conducted using our NeuroimagingPheWAS Matlab toolbox (http://bd2k.ini.usc.edu/tools/neuroimaging-phewas/), which is developed based on the free SurfStat package (http://www.math.mcgill.ca/keith/surfstat/). The break point analysis was performed using the package "Segmented" in R (Muggeo 2008) (https://cran.r-project.org/web/packages/segmented/index.html). The group-sparse block PCA was implemented using the package "sparse PCA" in R (https://github.com/chavent/sparsePCA).

Results

Sample Characteristics

The current sample of 8 137 participants is a group of generally healthy middle-aged and older adults (range 45.17–79.37 years,

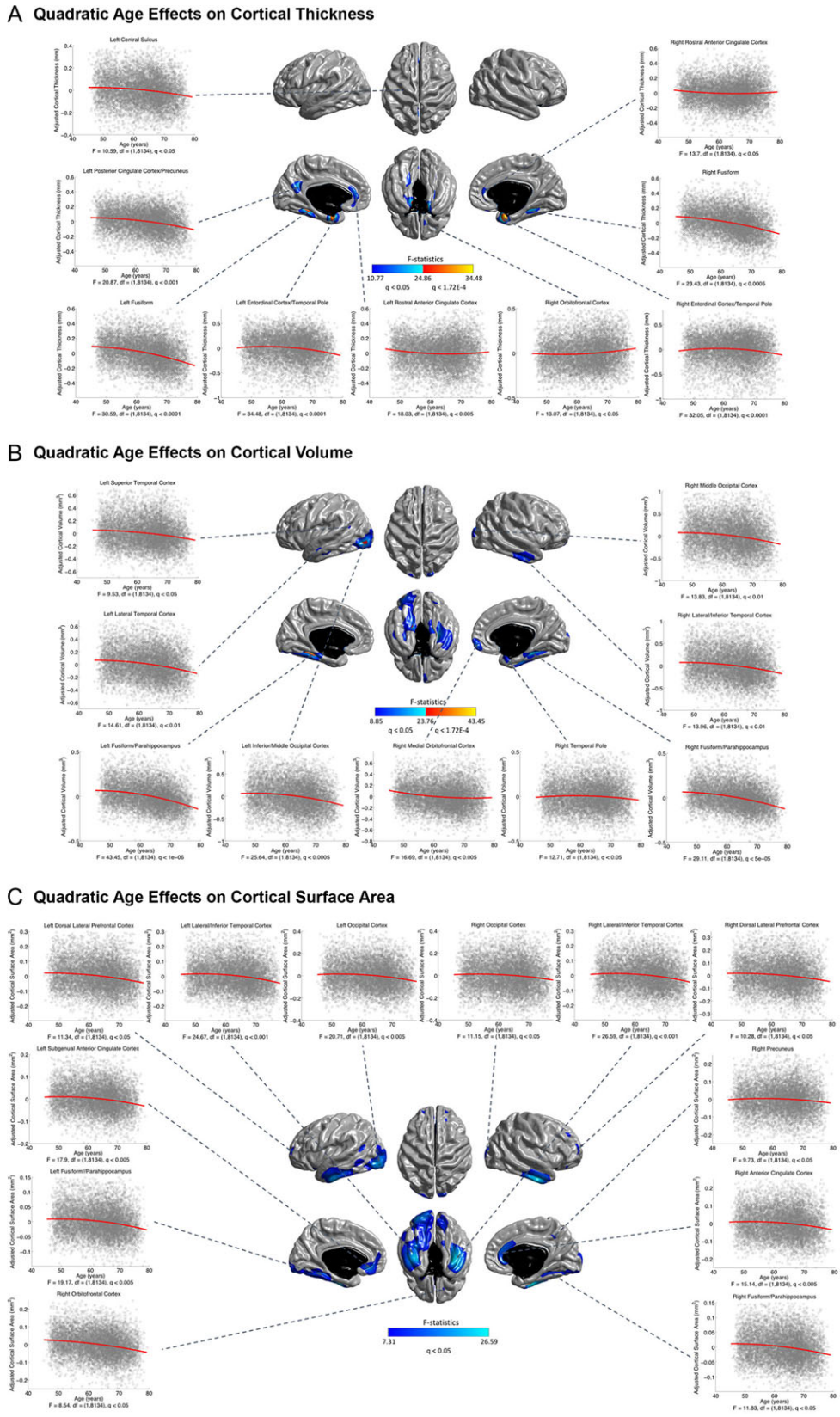

Figure 1. Quadratic age effects on cortical thickness (CTh) (*A*), volume (CVo) (*B*), and surface area (CSA) (*C*) throughout the cerebral cortex. Color bar represents *F*-statistics. Areas in blue-cyan represent patterns at the exploratory level of $q < 0.05$, areas in red-yellow represent patterns at the conservative level of $q < 1.72E\text{-}4$. Fitted quadratic trajectories are depicted for vertices with maximum *F*-statistics in clusters (*x*-axis = age (years), *y*-axis = cortical morphological measures adjusted for sex and intracranial volume).

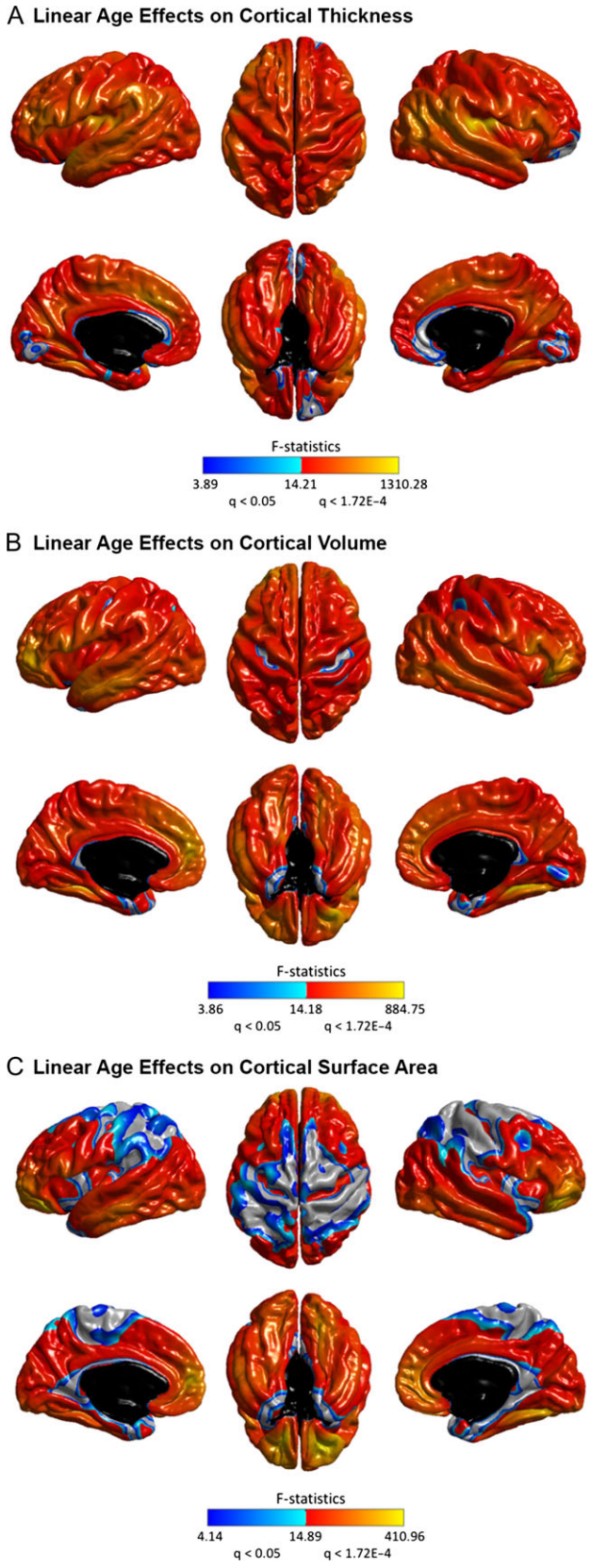

Figure 2. Linear age effects on CTh (*A*), CVo (*B*), and CSA (*C*) throughout the cerebral cortex. Color bar represents *F*-statistics. Areas in blue-cyan represent patterns at the exploratory level of $q < 0.05$, areas in red-yellow represent patterns at the conservative level of $q < 1.72E\text{-}4$.

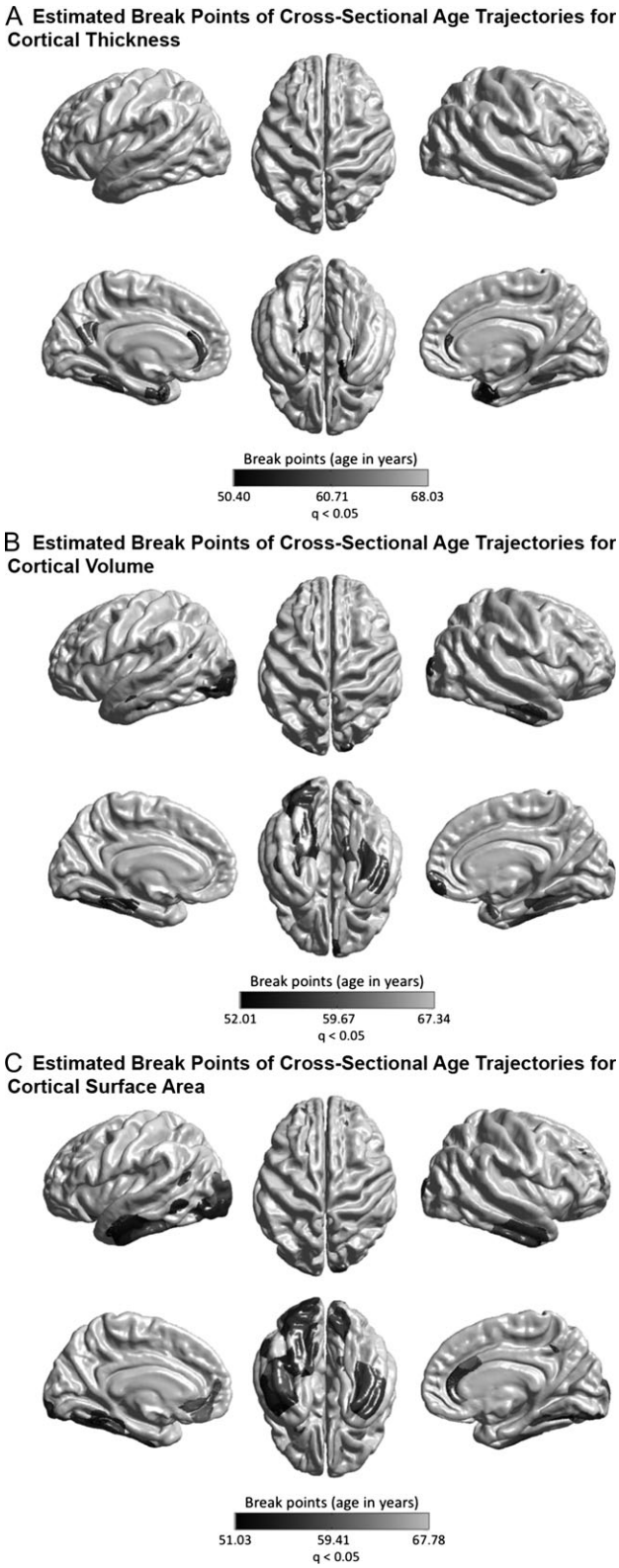

Figure 3. Estimated break points (at the exploratory level of $q < 0.05$) for the associations between age and CTh (*A*), CVo (*B*), and CSA (*C*) in the regions showing a quadratic age effect. The results at the conservative level of $q < 1.72E\text{-}4$ are shown in Supplementary Fig. S1.

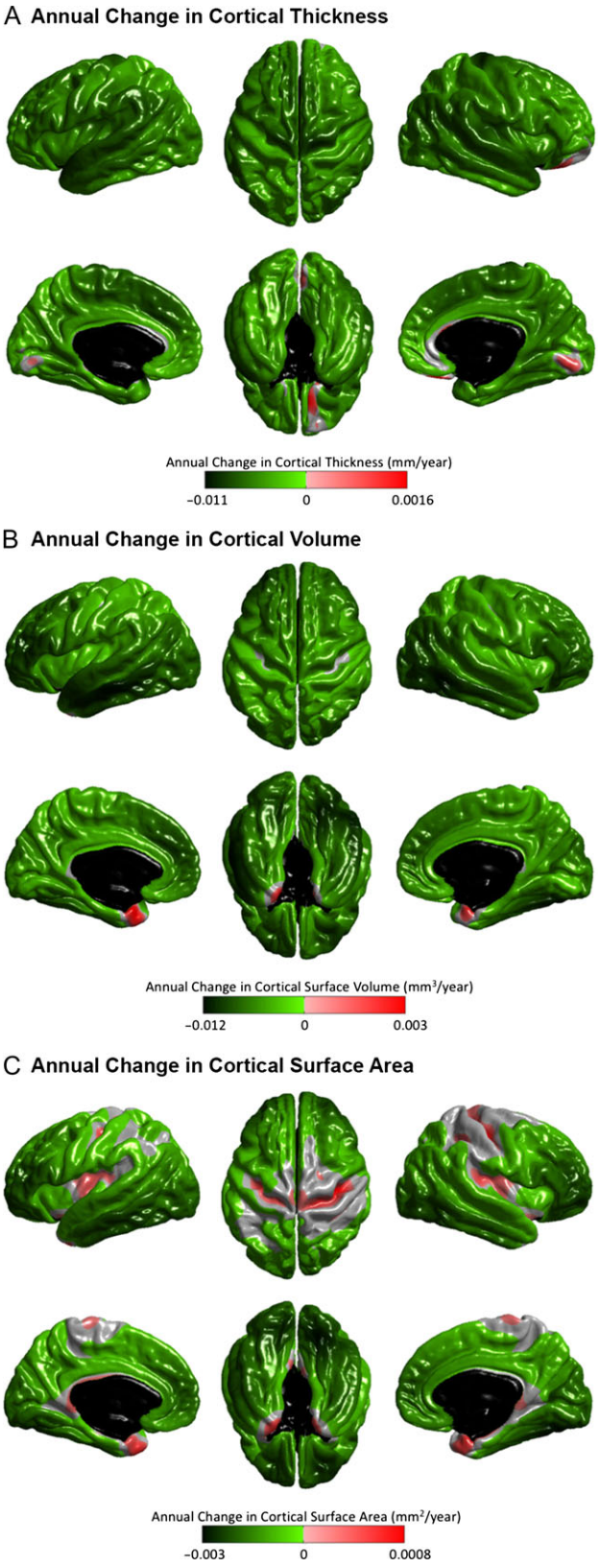

Figure 4. Annualized changes in CTh (*A*), CVo (*B*), and CSA (*C*), computed from the fitted generalized linear regression models with sex and intracranial volume as confounding factors. Only effects that survived FDR correction for multiple comparisons at the 0.05 level are displayed. Green-lime reflects decreases and pink-red reflects increases.

mean age = 62.69 ± 7.44 years) and consisted of 3882 males (47.71%). Table 1 further describes the statistics of basic demographic variables, cognitive tests, lifestyle behaviors, and genotypes of the APOE and the haplotype KL-VS of KLOTHO. The SNPs of the target genetic factors are summarized in Table 2.

Complex Age Effects on Cortical Morphology

The linear and nonlinear age effects at each vertex for the three structural measures—CTh, CVo, and CSA are illustrated in Figures 1 and 2. At the exploratory level of $q < 0.05$, quadratic age effects were found in several limbic/paralimbic areas, including the medial orbitofrontal cortex (mOFC), the medial temporal cortex (mTC), and the cingulate cortex, for all measures. Extra quadratic age effects were observed in the lateral temporal cortex (LTC) and occipital regions for CVo and CSA, and in the dorsolateral prefrontal cortex (DLPFC) for CSA. Especially, the quadratic age effects in the left mTC and the bilateral temporal poles for CTh, and in the left mTC and the left lateral occipital cortex (LOC) for CVo survived the conservative correction for multiple comparisons at $q < 1.72E\text{-}4$. The break point analysis using segmented regression showed that the mean cross-sectional age trajectories in the regions with quadratic age effects changed in slope at age of 60.12 ± 3.16 years for CTh, 59.19 ± 2.68 years for CVo, and 59.16 ± 3.01 years for CSA (at the exploratory level of $q < 0.05$) (Fig. 3). The existence of the break points for the left mTC and posterior cingulate cortex (PCC) and the bilateral temporal poles for CTh, and for the bilateral mTC for CVo survived the conservative correction for multiple comparisons at $q < 1.72E\text{-}4$ as well (Supplementary Fig. S1). Figure 4 presents the annualized changes across the middle to old adult age range computed from the fitted linear regression models at each vertex for the structural measures. Negative associations between age and cortical morphology (at the exploratory level of $q < 0.05$) were found across most of the cortical areas, most pronouncedly in the prefrontal cortex (PFC) and LTC for all measures, additionally in the inferior parietal cortex (IPC) for CTh and in the inferior temporal cortex (ITC) and OFC for CVo and CSA. Most of these linear age effects also survived the conservative correction at $q < 1.72E\text{-}4$, except those in the superior parts of the left precentral gyrus (PreCG) and postcentral gyrus (PostCG) and the superior and inferior parietal cortex for CSA (Fig. 2). No cubic age effect on any of the measures were found across the cortex.

Potential Modifiers of Age-Related Cortical Differences

Demographics

At the exploratory level of $q < 0.05$, sex effects on the age-differences in CTh were detected in the DLPFC, central motor cortex (CMC), cingulate cortex, bilateral lingual gyri (LING), the left lateral orbitofrontal cortex (LOFC), and the right ITC and posterior insula (Fig. 5A). In these areas, males showed greater negative associations between age and cortical morphology than females. Such sexual dimorphisms largely expanded to most of the cortical mantle for CVo and CSA (at the exploratory level of $q < 0.05$), except the bilateral triangular parts of the inferior frontal gyri (IFG), insula, the bilateral temporal poles (TPO), the left intraparietal cortex (iPC) and posterior middle temporal cortices (MTC), the right superior temporal cortex (STC), the upper portion of the precuneus, and the anterior parahippocampus (Fig. 5B,C). The sex effects in the bilateral PreCG and lower PoCG, the left LTC, anterior PFC and medial

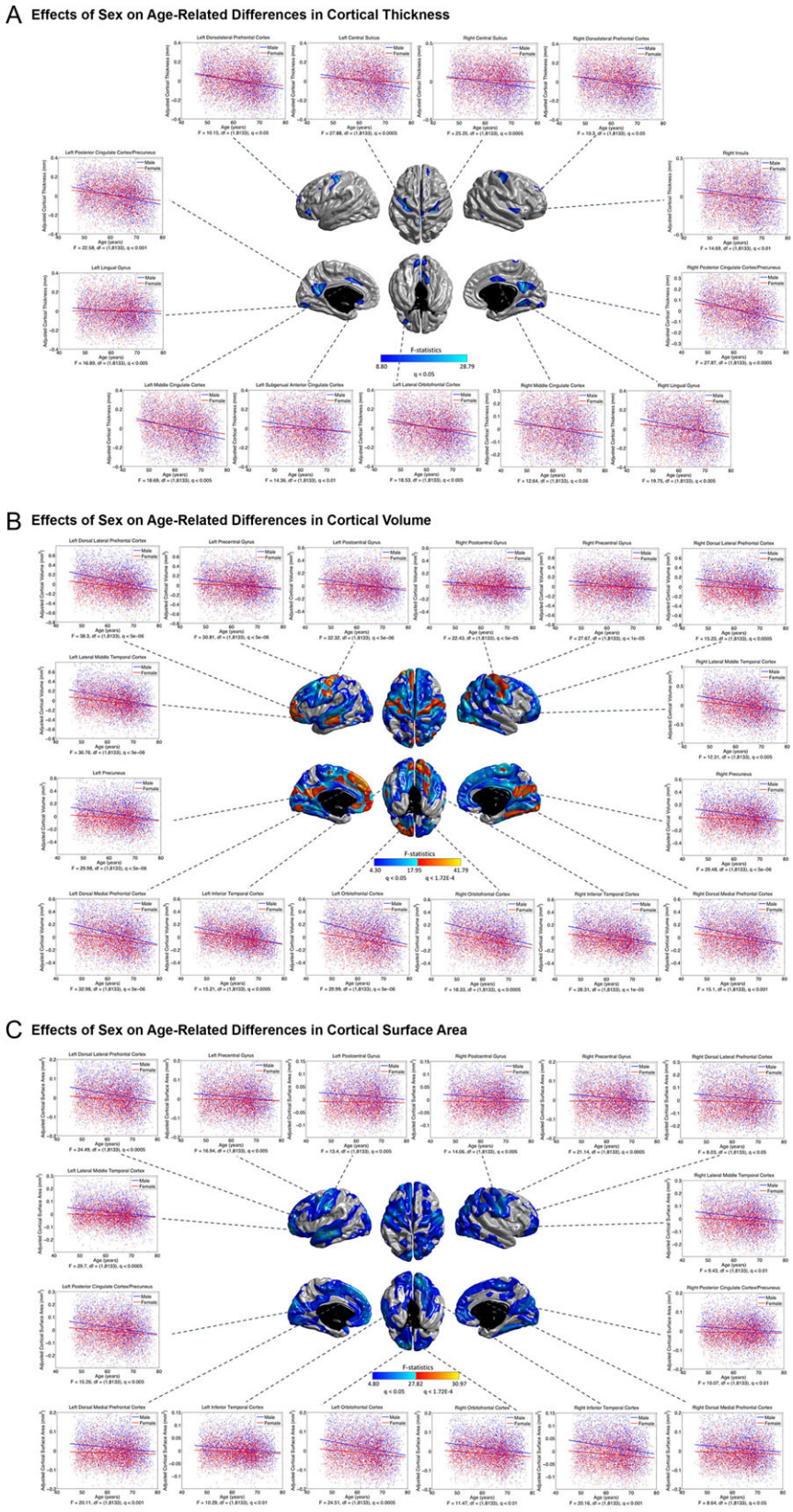

Figure 5. Sex effects on age-related differences in CTh (*A*), CVo (*B*), and CSA (*C*). Color bar represents *F*-statistics. Areas in blue-cyan represent patterns at the exploratory level of $q < 0.05$, areas in red-yellow represent patterns at the conservative level of $q < 1.72E\text{-}4$. Fitted age trajectories for males (blue lines) and females (red lines) are depicted for vertices with maximum *F*-statistics in clusters (*x*-axis = age (years), *y*-axis = cortical morphological measures adjusted for intracranial volume).

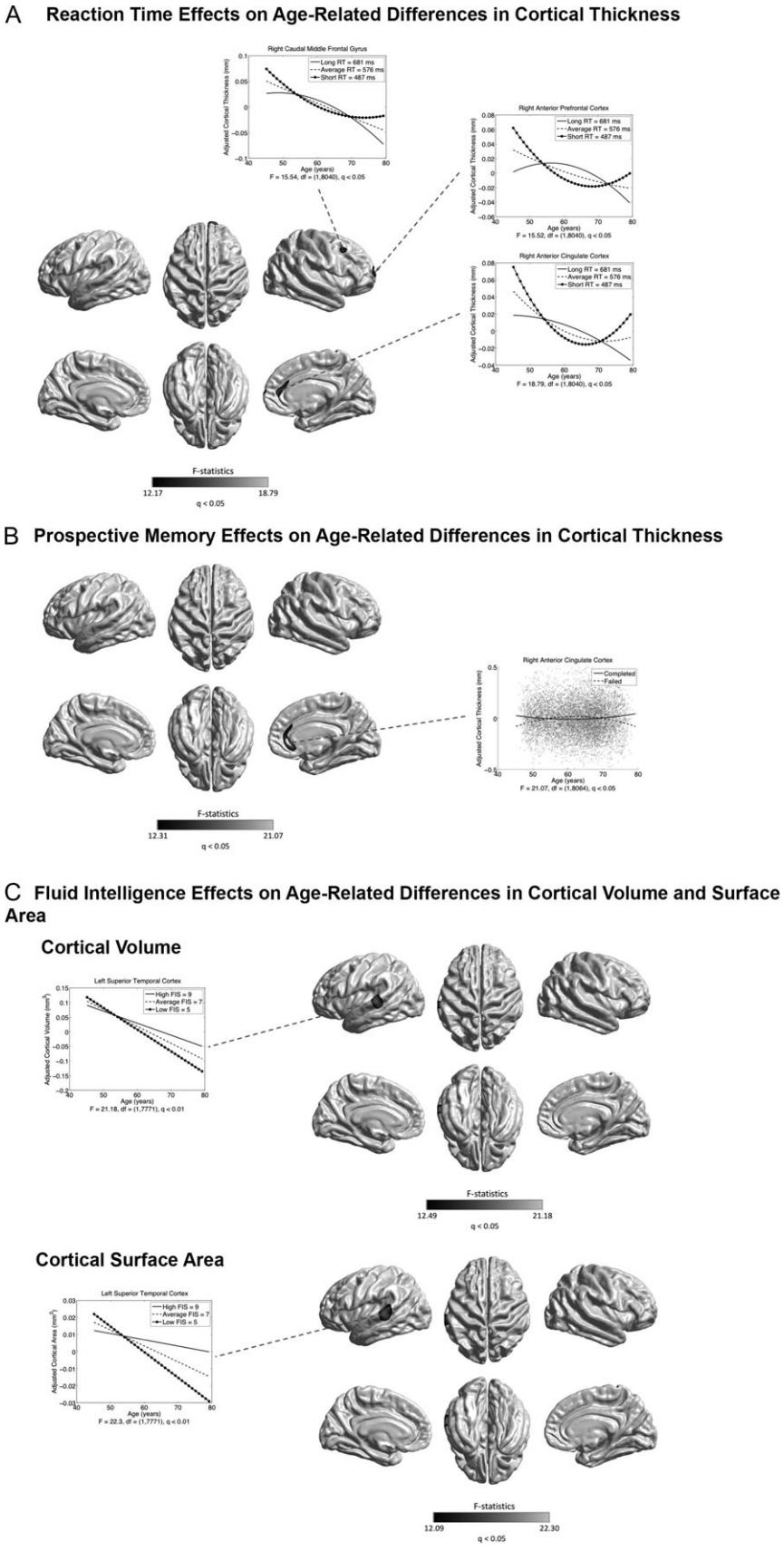

Figure 6. Associations between cognitive performance and age-related cortical morphological differences. Grayscale bar represents *F*-statistics. Areas in black-lightgray represent associations at the exploratory level of $q < 0.05$. (A) Associations between reaction time (RT) and age-related CTh differences. Because RT were

prefrontal cortex (mPFC), the bilateral PCC, paracentral lobules (PCL), mTC and LING, and the right angular gyrus (ANG) for CVo, and in a small region at the left LTC for CSA also survived the conservative correction at $q < 1.72E\text{-}4$. We observed no association between education qualifications and age-related cortical differences for all measures.

Cognitive Functions

Negative associations between age and cognitive functions in the studied sample were detected using all the cognitive tests (Supplementary Fig. S2). The performance of the cognitive tests was also found to be correlated with brain morphology in multiple prefrontal and temporal regions (Supplementary Figs S3–S6). Associations of cognitive functions with age-related cortical differences identified at the exploratory level of $q < 0.05$ were illustrated in Figure 6. The nonlinearity of CTh–age relationship was found to vary with the variation in reaction time in the right anterior cingulate cortex (ACC), caudal MTC, and anterior PFC (Fig. 6*A*). A similar pattern was seen for prospective memory in the right ACC (Fig. 6*B*). Decreased fluid intelligence score was associated with a greater negative association between age and CVo/CSA in the left STC (Fig. 6*C*). None of these effects of cognitive functions on age-related cortical differences survived the conservative correction at $q < 1.72E\text{-}4$. No association of visual memory performance with age-related cortical differences was detected.

Smoking

Current and ex-smokers showed a widespread cortical morphometric reduction (pronounced for CTh and CVo) relative to those who had never smoked (Supplementary Figs S7–S9). Current smokers also showed smaller CVo in the left parahippocampus and ITC compared with ex-smokers (Supplementary Fig. S8*C*). Within current and ex-smokers ($n = 2005$), we found negative widespread correlations of pack-years with cortical morphology (Supplementary Fig. S10). Assessing associations of smoking status with age-related cortical differences found a greater negative association between age and CVo in current smokers compared with those who had never smoked (at the exploratory level of $q < 0.05$), in the IFG, ACC, and middle cingulate cortex (MCC), the left subcentral cortex (SCC), the right LOC, the right precuneus, and parahippocampus (Fig. 7). These effects of smoking status on age-related CVo differences did not survive the conservative correction at $q < 1.72E\text{-}4$. No smoking status effects were found on age-related differences in CTh and CSA. In smokers, the number of cigarettes smoked per day was not associated with age-related cortical differences, no matter if duration of smoking was adjusted.

Alcohol Consumption

In the sample consisted of both abstainers and alcohol drinkers, a U-shaped relationship of alcohol consumption with CTh and CVo was found in widespread brain regions (Supplementary Fig. S11). These results still remained when abstainers were excluded. At the exploratory level of $q < 0.05$, compared with abstainers, individuals consuming >30 drinks/week showed a greater negative association between age and CVo in the CMC, pre-motor cortex (PMC), mTC, rostral ACC, and occipital cortex, and the left LOFC and STC, and the right MCC and temporoparietal junction (TPJ) (Fig. 8*B*). Some of these patterns, for example, in the STC and mTC, were consistent also for CTh and CSA (Fig. 8*A*,*C*). Increased negative CVo–age associations in the left parahippocampus and the right superior frontal gyrus (SFG) were also observed in individuals consuming 14–21 and 21–30 drinks/week, respectively (at the exploratory level of $q < 0.05$) (Supplementary Fig. S12). None of the alcohol consumption effects on age-related cortical differences survived the conservative correction at $q < 1.72E\text{-}4$.

Sleep

Associations of insomnia status with age-related morphological differences identified at the exploratory level of $q < 0.05$ are illustrated in Figure 9. Frequent insomnia symptoms were associated with an inverted U-shaped CVo–age relationship in the mPFC, IFG, SFG, LING, the left STC, the right CMC, PMC, superior parietal cortex (SPC), rolandic operculum (ROL), precuneus, posterior parahippocampus, and anterior insula (Fig. 9*B*). Most of these patterns were consistently observed for CSA, except the ones in the LING and the right precuneus, parahippocampus, anterior insula, and SPC (Fig. 9*C*). A CTh effect was found in the left LING (Fig. 9*A*). These effects of insomnia status on age-related cortical differences did not survive the conservative correction at $q < 1.72E\text{-}4$. No effects of sleep duration on age-related morphological differences were found, neither using the raw continuous nor the categorized (short: <7 h, average: 7–9 h, long: >9 h) measures.

Genetics

In the whole sample, no genetic association with age-related cortical differences was found, except between the BDNF Val66Met SNP (rs6265) and age-related CSA difference in the left SMG (at the exploratory level of $q < 0.05$) (Supplementary Fig. S13). Previous cognitive data have reported that effects of potential genetic modifiers for brain aging, for example, APOE, may be more pronounced at older ages (Schiepers et al. 2012; Davies et al. 2015; Marioni et al. 2016). Therefore, we repeated the analyses dividing the current sample into an older subsample (>60 years, $n = 5273$) and a younger subsample (≤60 years, $n = 2864$). In the older subsample, associations (at the exploratory level of $q < 0.05$) were found between APOE and age-related CTh differences in the right mTC and PCC (Fig. 10*A*); between the BDNF Val66Met SNP (rs6265) and CVo differences in the left CMC, DLPFC, PCL, and the left parahippocampus and SMG (Fig. 10*B*); between the COMT Val158Met SNP (rs4680) and age-related CTh differences in the right DLPFC, CMC, parietal, MCC, and PCC (Fig. 10*C*); between the AD GWAS loci CASS4 (rs7274581) and age-related CSA differences in the right PoCG (Fig. 10*D*); and between the AD GWAS loci CD2AP (rs10948363) and age-related CSA differences in the right DLPFC, mPFC, OFC, and posterior MCC, and PreCG (Fig. 10*E*). In the younger

positively skewed, the variables were transformed with a log transform. Fitted age trajectories for average RT (mean(RT) = 576 ms) (dashed lines), long RT (mean(RT) + SD(RT) = 681 ms) (solid lines), and short RT (mean(RT) − SD(RT) = 487 ms) (circle, solid lines) are depicted for vertices with maximum *F*-statistics in clusters (*x*-axis = age (years), *y*-axis = CTh adjusted for sex and intracranial volume). (*B*) Associations between prospective memory performance and age-related CTh differences. Fitted age trajectories for participants who completed the task on first attempt (solid line) and failed (dashed line) are depicted for the vertex with maximum *F*-statistic in the cluster. (*C*) Associations between fluid intelligence score (FIS) and age-related differences in cortical volume (CVo) (top panel) and CSA (bottom panel). Fitted age trajectories for average FIS (mean(FIS) = 7) (dashed lines), high FIS (mean(FIS) + SD(FIS) = 9) (solid lines), and low FIS (mean(FIS) − SD(FIS) = 5) (circle, solid lines) are depicted for vertices with maximum *F*-statistics in clusters.

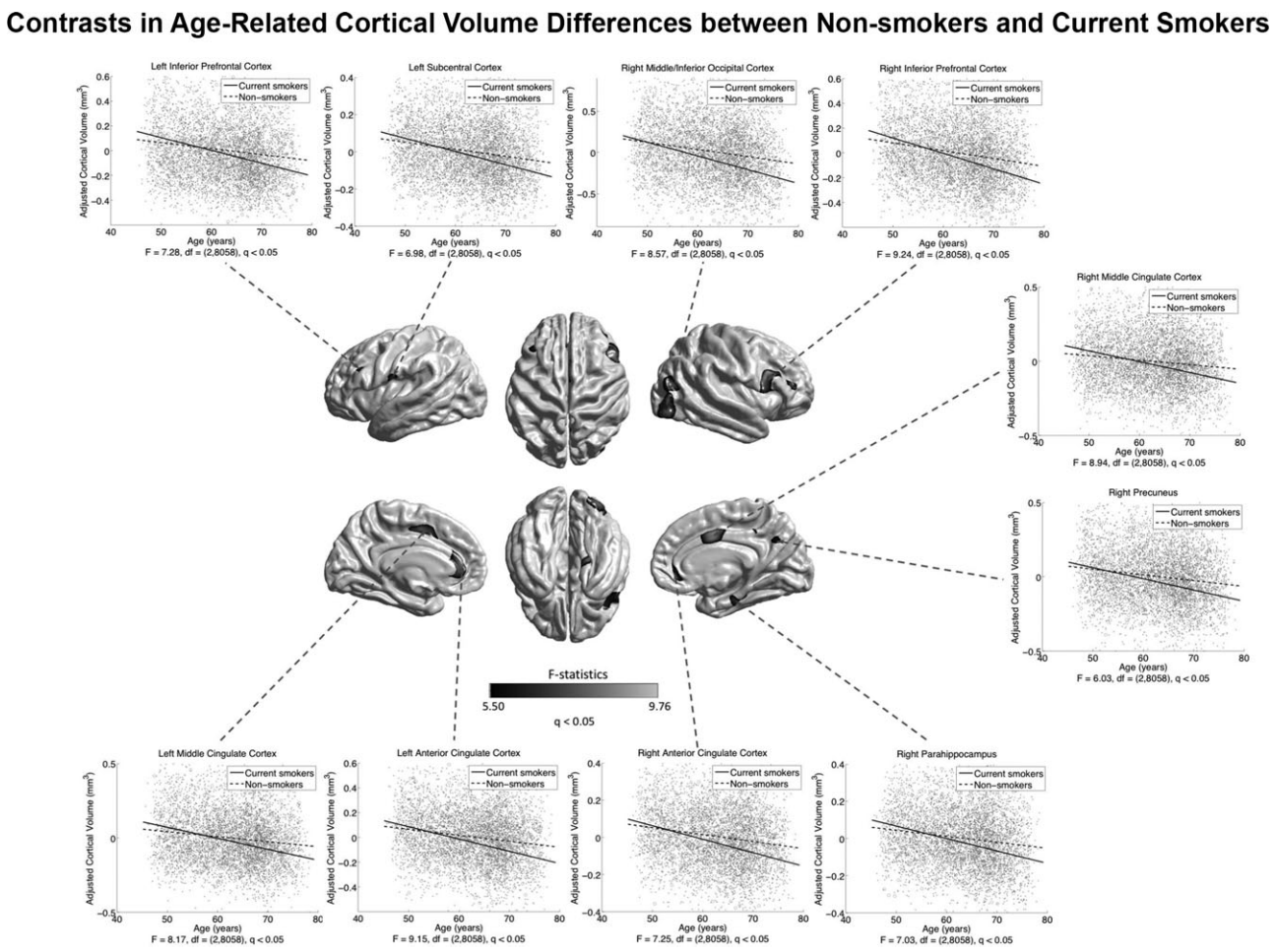

Figure 7. Differences between current smokers and lifetime nonsmokers in age-related CVo differences. Grayscale bar represents *F*-statistics. Areas in black-lightgray represent patterns at the exploratory level of $q < 0.05$. Fitted age trajectories for lifetime nonsmokers (dashed lines) and current smokers (solid lines) are depicted for vertices with maximum *F*-statistics in clusters (*x*-axis = age (years), *y*-axis = CVo adjusted for sex and intracranial volume).

subsample, age-related CTh differences were associated with the AD GWAS loci MEF2C (rs190982) in the left DLPFC, LOFC, SCC, iPC, LTC, TPO and fusiform regions, and the right STC and IFG (at the exploratory level of $q < 0.05$) (Fig. 11*A*); and with the AD GWAS loci DSG2 (rs8093731) in the left occipital cortex (at the exploratory level of $q < 0.05$) (Fig. 11*B*). None of these genetic effects on age-related cortical differences survived the conservative correction at $q < 1.72E\text{-}4$. No association of the *KLOTHO* gene (haplotype KL-VS) with age-related cortical differences was found in the whole sample or subsamples.

Joint Effects of Cognitive, Lifestyle Variables, and Education

The loadings of the first 10 PCs that were derived by the group-sparse block PCA and together explained over 95% of variance among the original multivariate data are presented in Table 3. Analyzing the interactions between these PCs and age on cortical morphemtrics, the third PC (notated as PC3) showed diffuse associations with age-related CTh differences in the bilateral central sulci, the left STC, the right ITC, LING and ventromedial prefrontal cortex (vmPFC) (at the exploratory level of $q < 0.05$) (Fig. 12*A*); and the fifth PC (PC5) was associated with age-related CVo differences in the right precuneus (at the exploratory level of $q < 0.05$) (Fig. 12*B*). In these patterns, lower PC3 and PC5 scores were correlated with a greater negative association between age and cortical morphology. PC3 was a combined variable of insomnia status (|loading| = 0.59), alcohol drinker status (|loading| = 0.31), sleep duration (|loading| = 0.24), alcohol consumption (|loading| = 0.16), prospective memory (|loading| = 0.1), and education, smoking status and pack-years of smoking (|loading| < 0.1), and explained 12.58% of variance in the multivariate data; PC5 was a combination of prospective memory (|loading| = 0.51), education (|loading| = 0.47), and fluid intelligence, smoking status, pack-years of smoking and alcohol drinker status (|loading| < 0.10), and explained 10.55% of variance. The PC3 and PC5 effects did not survive the conservative correction at $q < 1.72E\text{-}4$. No associations of the other PCs with age-related morphological differences were found.

Discussion

This study adds to our understanding of age-related differences in brain morphology in healthy middle-aged and older adults. The distribution of linear and nonlinear associations between age and brain morphology across the brain was found to be related to the laminar organization and evolutionary history of the cortex. Age of about 60 years was found to be a break point for increasing negative associations between age and brain morphology in the AD-prone areas. Further, individual effects of sex, cognitive functions, lifestyle behaviors, specific genetic

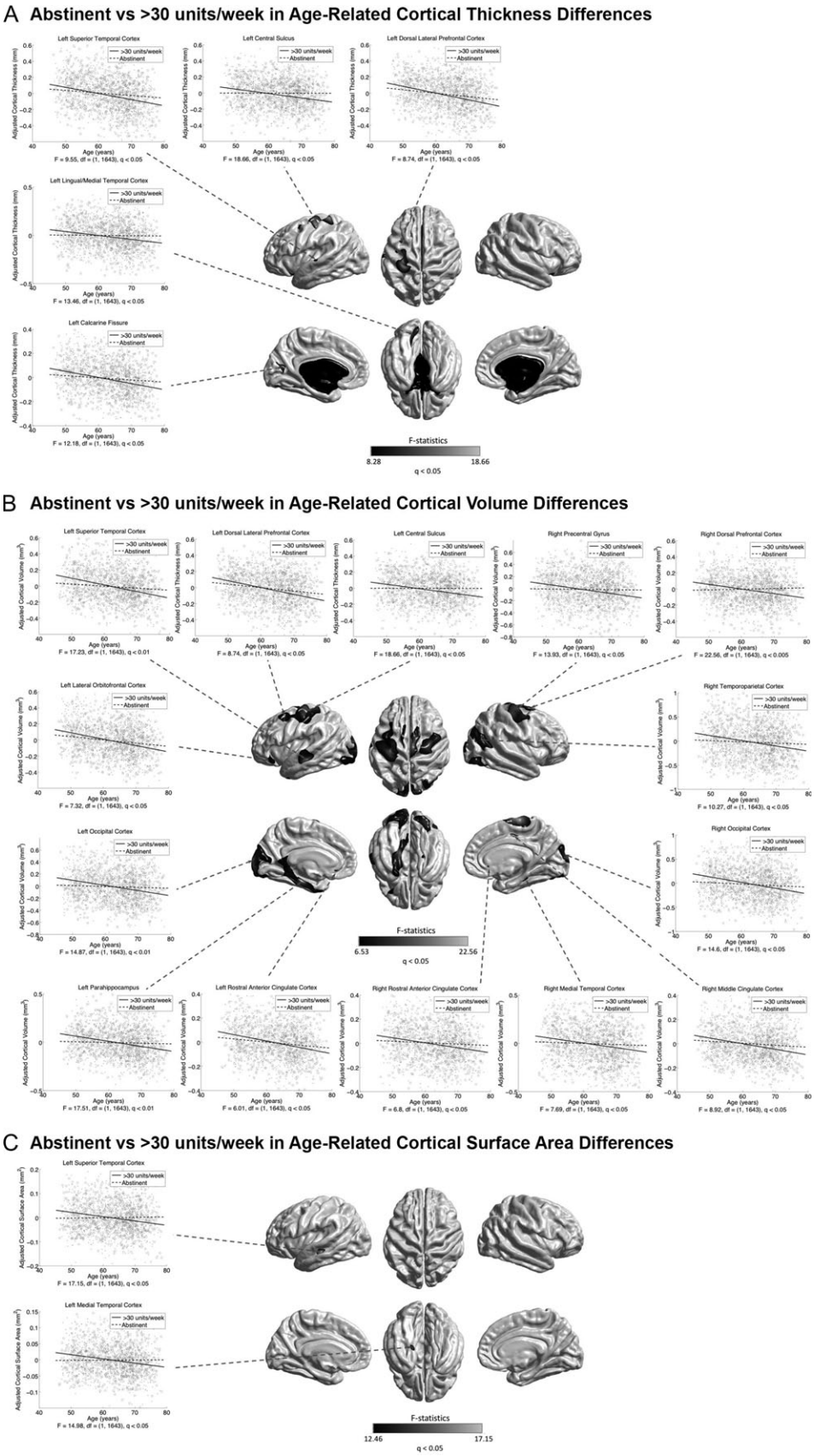

Figure 8. Differences between heavy alcohol drinkers (>30 standard drinks/week) and abstainers in age-related differences in CTh (*A*), CVo (*B*), and CSA (*C*). Grayscale bar represents *F*-statistics. Areas in black-lightgray represent patterns at the exploratory level of $q < 0.05$. Fitted age trajectories for abstainers (dashed lines) and heavy drinkers (solid lines) are depicted for vertices with maximum *F*-statistics in clusters (*x*-axis = age (years), *y*-axis = cortical morphological measures adjusted for sex and intracranial volume).

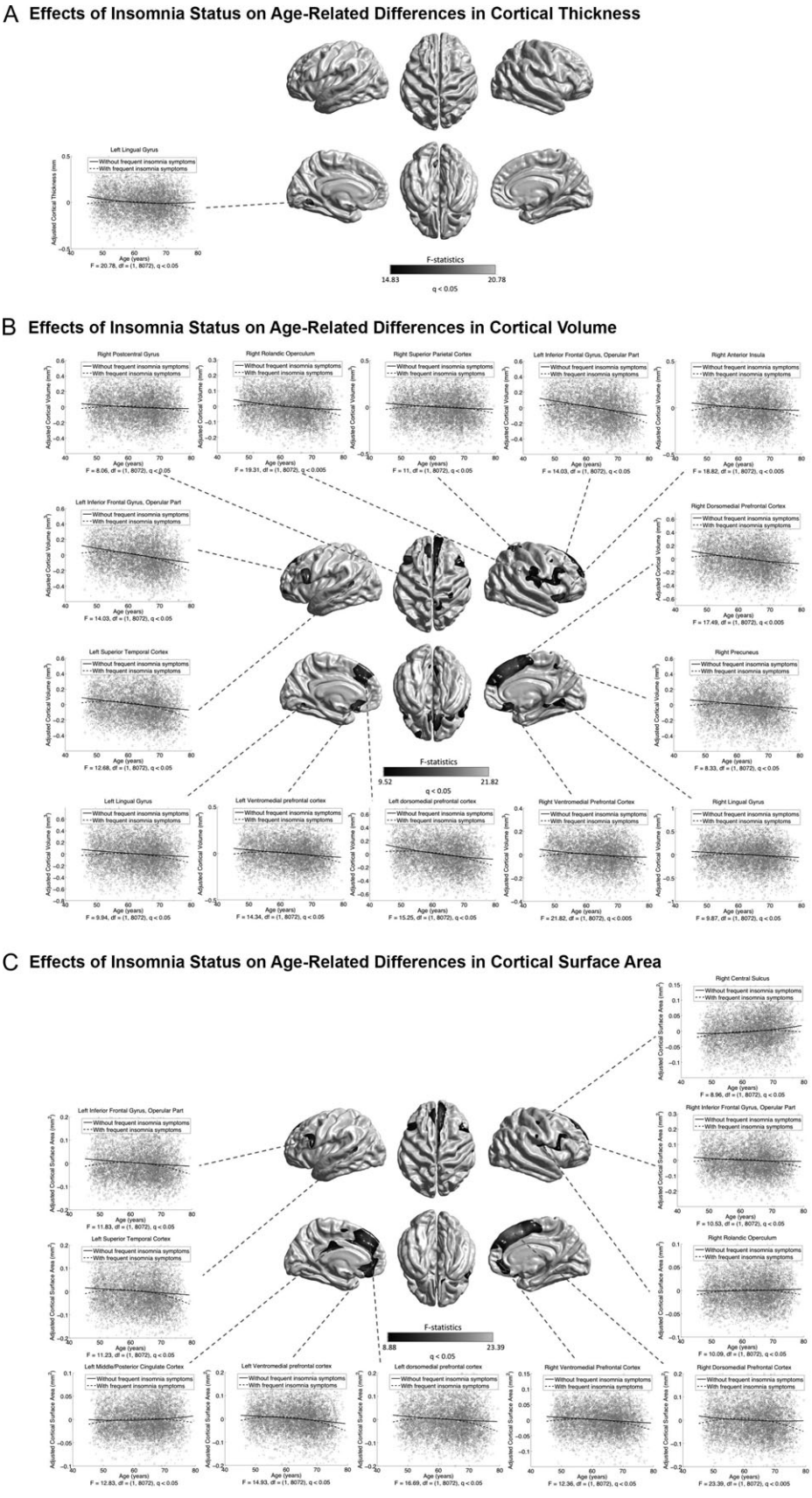

Figure 9. Associations between insomnia status and age-related differences in CTh (*A*), CVo (*B*), and CSA (*C*). Grayscale bar represents *F*-statistics. Areas in black-lightgray represent patterns at the exploratory level of $q < 0.05$. Fitted age trajectories for individual with frequent insomnia symptoms (dashed lines) and without frequent insomnia symptoms (solid lines) are depicted for vertices with maximum *F*-statistics in clusters (*x*-axis = age (years), *y*-axis = cortical morphological measures adjusted for sex and intracranial volume).

factors and combined effects of the cognitive, lifestyle variables, and education on age-related cortical differences were identified systematically.

Complex Cortical Morphology–Age Associations Align with Laminar Cortical Organization

The current large cross-sectional SBM study revealed remarkable quadratic age effects in several limbic/paralimbic areas (mOFC, mTC, ACC, and PCC) consistently for CTh, CVo, and CSA (Fig. 1). Especially, the quadratic age effects in the left mTC for CTh and CVo survived the conservative correction for multiple comparisons at $q < 1.72E\text{-}4$. The limbic/paralimbic system is typically defined as the allocortex (3–4 cell layers) cytoarchitecturally (Zilles et al. 2015). In most of the remaining cortical mantle that are six-layered neocortex, only linear age effects were detected most pronouncedly in the PFC and LTC for all measures (Figs 2 and 4 and Supplementary Fig. S14) (at both exploratory level of $q < 0.05$ and conservative level of $q < 1.72E\text{-}4$). We also observed spared cortical structures with age especially in the central sulcus and surrounding areas for CVo and CSA (Figs 2 and 4). These findings are well in line with the cross-sectional (Ziegler et al. 2012; Fjell et al. 2014) and longitudinal data (Storsve et al. 2014) from recent cortical morphometry studies, as well as with the predominant vulnerability of prefrontal and temporal white matter (WM) to the deleterious effects of aging reported by previous WM volume studies (Gunning-Dixon et al. 2009; Salat et al. 2009; Fjell and Walhovd 2010). The neurobiological basis for differential cortical changes in normal aging remain unclear. Previous neuroimaging studies have revealed a parallel between basic types of the cortex and the patterns of cortical development during childhood through early adulthood: nonlinear developmental trajectories were mainly located in neocortex areas (Gogtay et al. 2004; Lenroot et al. 2007; Shaw et al. 2008), whereas linear growth trajectories predominantly were located in the allocortex structures (Shaw et al. 2008). Our findings, together with the existing morphometry data (Ziegler et al. 2012; Fjell et al. 2014; Storsve et al. 2014), show that the patterns of age-related cortical differences or changes in normal aging also align closely with the laminar organization of the cortex: the neocortex largely follows a linear trajectory, while allocortex mainly follows a curvilinear path. Such alignment in aging appears to follow the inverse of neurodevelopment (Pfefferbaum et al. 2013). The allocortex and neocortex are the 2 broad cortical types identified by comparisons of cortical organizations across several species, that is, allocortex areas are homogenous in all mammalian brains and thus likely evolved in early mammals, whereas many of neocortex areas are unique to primates indicating a later evolution (Striedter 2006). Therefore, the combined findings in normal neurodevelopment and aging suggest a possible evolutionary program for the complexity of differential structural brain changes across the life span.

Furthermore, in line with previous findings (Dickerson et al. 2009; Storsve et al. 2014), age-related CVo differences appear largely related to CSA differences in temporal cortices as well as in occipital areas, while CTh differences were partially responsible for the late-life increased CVo–age association in the fusiform (Figs 1 and 2). It has been suggested that CSA increases might contribute to brain connectivity development than CTh increases (Murre and Sturdy 1995), and that pruning in childhood and adolescents is a prerequisite for optimal CSA increases (White et al. 2010). Thus, age-related cortical shrinkage is not a uniform process but rather is the result of separate mechanisms of CTh and CSA changes in separate anatomical regions (Storsve et al. 2014). This further highlights the need to take multiple measures of cortical morphology into consideration to obtain a better understanding of the neurobiological processes that characterize normal aging.

Age of About 60 is the Break Point for Increasing Negative Cortical Morphology–Age Association

The quadratic cross-sectional age trajectories estimated in the current study suggest an increase in negative associations between age and cortical morphological measures after around 60 years in the bilateral temporal cortices as well as in the left PCC/precuneus (pronounced for CTh), occipital cortices (pronounced for CVo and CSA), and DLPFC (pronounced for CSA) (Fig. 1). We conducted a break point analysis using segmented regression modeling (Muggeo 2003; 2016). The results confirmed that the changes in the slopes of the associations between age and brain morphology in the regions with a quadratic age effect occurred at the age of around 60 years (60.12 ± 3.16 years for CTh, 59.19 ± 2.68 years for CVo, and 59.16 ± 3.01 years for CSA) (Fig. 3), especially the existence of the break points for the mTC (for both CTh and CVo) and the left PCC (for CTh) survived the conservative correction at $q < 1.72E\text{-}4$ (Supplementary Fig. S1). A number of previous cross-sectional (Ziegler et al. 2012; Fjell et al. 2014) and longitudinal (Storsve et al. 2014) structural MRI studies have also reported increased negative associations between age and brain morphology or accelerated cortical declines after about 60 years in these areas, although few of them statistically tested this observation. Some life span diffusion-weighted magnetic resonance imaging (DWI) data reported that diffusion tensor measures of WM (global fractional anisotropy [FA], mean diffusivity [MD], and radial diffusivity [RD]) peaked at around 30 years, followed by a small, yet stable, decrease/increase until about 60 years with a subsequent accelerated decrease/increase (Westlye et al. 2010). In line with this, another recent study on age-related WM differences in 3513 UK Biobank participants reported increased adverse associations of age with MD and neurite orientation dispersion and density imaging (NODDI) measures (intracellular volume fraction [ICVF], isotropic volume fraction [ISOVF], and orientation dispersion [OD]) of most major WM tracts after about 60 years. In addition, we found increased negative associations between age and fluid intelligence and prospective memory performance after around 60 years in the current sample (estimated break point for fluid intelligence = 63.85 years, uncorrected $P = 1.69E\text{-}8$; estimated break point for proportion of success in prospective memory = 60–65 years, uncorrected $P = 0.038$) (Supplementary Fig. S1). Merging these multimodal imaging and cognitive data, we speculate that age of about 60 years may be the break point for accelerated cortical declines in normal aging. Furthermore, temporal cortices, such as the entorhinal cortex (EC), parahippocampus, LTC and fusiform, and the PCC are known to be vulnerable in AD, and the pathological atrophy likely appears years before clinical symptoms (Davatzikos et al. 2009; Jack et al. 2010). It was suggested that accelerating atrophy in these AD-prone areas may be caused by undetected neurodegenerative diseases and is not a feature of healthy aging (Burgmans et al. 2009). Nevertheless, a recent study explicitly demonstrated that undetected AD could evidence nonlinearity in EC only, rather in the other AD-vulnerable regions (Fjell et al. 2014). Our cross-sectional analyses detected increasing associations between age and cortical morphology in all the AD-vulnerable temporal regions except EC. Therefore, preclinical conditions should have been well

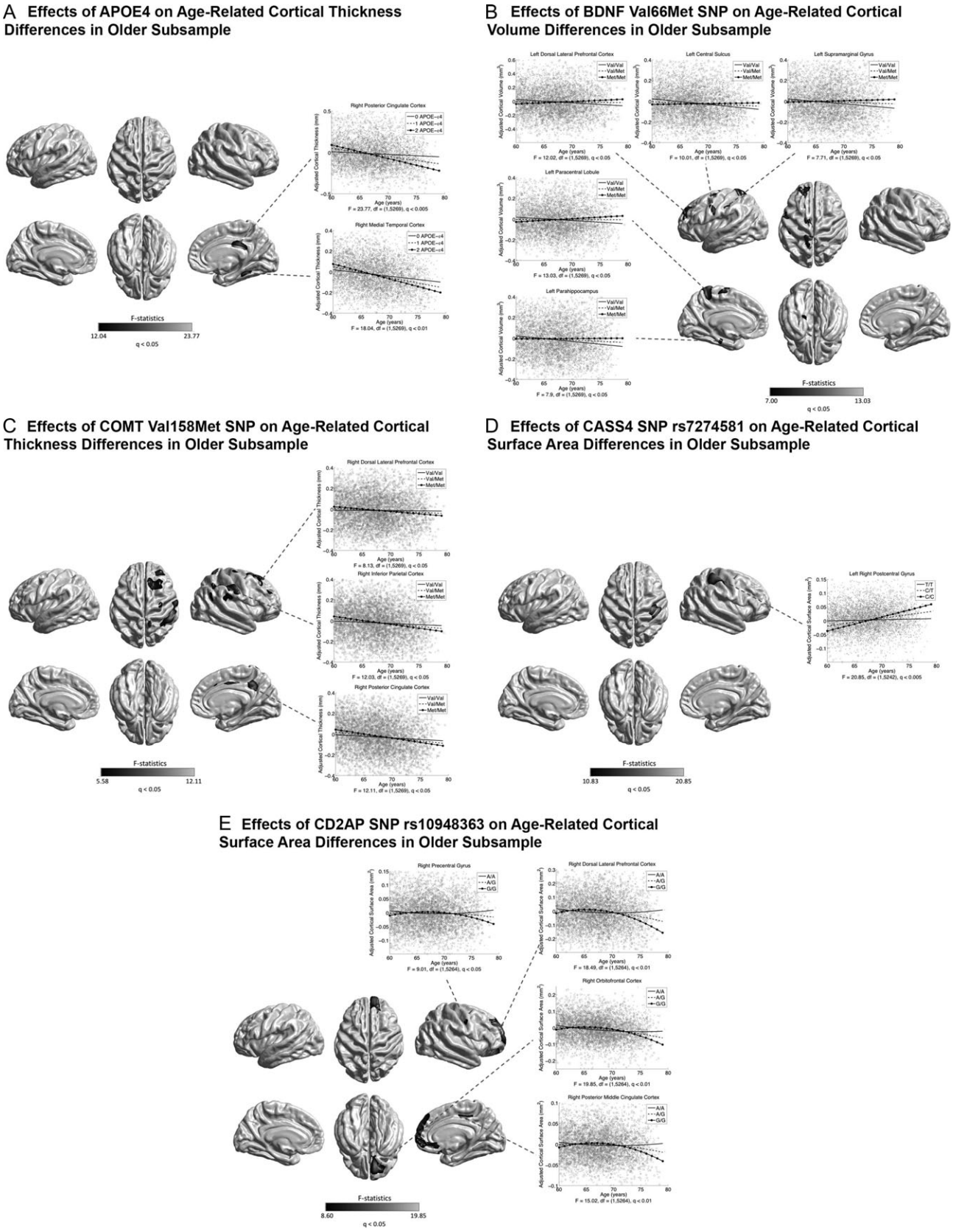

Figure 10. Associations between genetic variants and age-related cortical morphological differences in the older subsample (>60 years). Grayscale bar represents *F*-statistics. Areas in black-lightgray represent patterns at the exploratory level of $q < 0.05$. (*A*) Associations between APOE ε4 (risk for Alzheimer's disease [AD]) and age-related CTh differences. Fitted age trajectories for 0 (solid lines), 1 (dashed lines), and 2 (circle, solid lines) ε4 alleles are depicted for vertices with maximum *F*-statistics in clusters (*x*-axis = age (years), *y*-axis = CTh adjusted for sex and intracranial volume). (*B*) Associations between BDNF Val66Met and age-related CVo

excluded in the current study (see Methods and Supplementary Table S2), and the observed nonlinearity could be related to normal aging dynamics in the temporal cortices.

Greater Negative Cortical Morphology–Age Associations in Males than Females

The role of sex in brain aging is still controversial. This study observed greater negative CTh–age associations in the DLPFC, mPFC, CMC, cingulate cortex, LING, ITC, and posterior insula, in males compared with females at the exploratory level of $q < 0.05$ (Fig. 5A), in line with previous findings (Takahashi et al. 2011; Pfefferbaum et al. 2013). These patterns of sex differences enlarged into more widespread cortical regions for CVo and CSA, especially the patterns in the CMC, PFC, PCC, mTC, Moc, the left LTC and the right ANG for CVo and the left LTC for CSA survived the conservative correction at $q < 1.72E\text{-}4$ (Fig. 5B,C). These greater negative cortical morphology–age associations in males may be related to their more extended age-related reduction of brain metabolism than females (Malpetti et al. 2017) and may yield a neuroanatomical basis for the faster age-related cognitive declines in males (Gur and Gur 2002). The cause of sex differences in brain atrophy with aging is still unclear. Gonadal hormones may play a key role in the underlying mechanism. For example, the level of testosterone that may have neuroprotective properties steadily decreases with age in healthy male adults (Holland et al. 2011). Therefore, including sex hormones in future studies on sexual dimorphism is warranted.

Better Cognitive Performance is Related to Reduced Negative Cortical Morphology–Age Associations

Cognitive functions deteriorate with age (Reuter-Lorenz and Park 2010; Harada et al. 2013) (Supplementary Fig. S2). To date, there are few papers describing the effects of cognitive functions on age-related cortical morphological differences in healthy middle-aged and older adults. In this work, variations in reaction time and prospective memory performance were associated with a transformation of the U-shaped CTh–age relationship in the right ACC at the exploratory level of $q < 0.05$ (Fig. 6A,B). Functional neuroimaging studies have revealed a key role of the ACC for determining the processing time in reaction time tasks (Naito et al. 2000) and the performance in prospective memory tasks (Cona et al. 2015). The current (Supplementary Figs S3 and S4) and previous (Righart et al. 2013) MRI data also showed significant structure–cognition relationships with reaction time and prospective memory response in the ACC. It has been reported that cognitive exercise may induce short-term structural changes in the aging brain (Engvig et al. 2010) and that neurofeedback training in the ACC may induce long-term cortical changes and produce significant improvement in working memory and processing speed (Cannon and Lubar 2011). These functional and structural findings support the hypothesis that the increased CTh at late ages in the ACC, which was consistently observed in the current (Fig. 1) and previous studies (Thambisetty et al. 2010; Fjell et al. 2014; Storsve et al. 2014; Yang et al. 2016) is likely related to neuroplasticity at older ages (Engvig et al. 2010). Additionally, this study detected negative correlations of the fluid intelligence score with the slopes of CVo/CSA–age associations at the exploratory level of $q < 0.05$. Higher intelligence has been associated with larger structural measures primarily in the prefrontal and temporal cortices in the current (Supplementary Fig. S5) and previous works (Choi et al. 2008; Luders et al. 2009; Menary et al. 2013; Karama et al. 2014). Interestingly, the fluid intelligence effects on CVo/CSA–age associations were found only in the STC (Fig. 6C) that is an essential structure involved in auditory and language processing. This may be because that the fluid intelligence task in the UK Biobank protocol requires reading comprehension and verbal reasoning, in addition to inductive and deductive logic capabilities (Lyall et al. 2016). Therefore, the STC involved in language comprehension may play a key role for determining the performance in this particular fluid intelligence test.

Unhealthy Lifestyles are Related to Greater Negative Cortical Morphology–Age Associations

In the current UK Biobank cohort, we successfully reproduced previous findings (Davatzikos et al. 2009; Jack et al. 2010; Karama et al. 2015) of the diffuse negative impacts of chronic cigarette smoking on brain structures in nondemented aging adults (Supplementary Figs S7–S9) and of the diffuse dose-dependent negative association between smoking and CTh in old smokers (Supplementary Fig. S10). We further identified diffuse increased negative associations between age and brain morphology in current smokers compared to nonsmokers, at the exploratory level of $q < 0.05$, pronouncedly in several AD-prone areas (parahippocampus and PCC/precuneus) and cortical components of brain reward system (BRS) that are known to extend in substance use disorders (Fowler et al. 2007) (ACC and PFC) as well as the left SCC and the right occipital cortices (Fig. 7). These are consistent with the reported smoking-induced increases in regional longitudinal brain atrophy rates in a relatively small subsample of healthy elderly from the ADNI cohort (Durazzo et al. 2012). Additionally, in ex-smokers, the regions with greater negative CVo–age associations in current smokers compared with nonsmokers showed a trend of larger negative CVo–age associations than in nonsmokers and smaller than in current smokers (uncorrected $P<0.05$) (Supplementary Fig. S15), being supportive of the possible partial recovery effect of smoking cessation (Karama et al. 2015). Of note, none of these trends survived FDR correction. We also found that the daily dosage of smoking did not affect the age-related cortical differences in smokers, regardless of the duration of smoking. Considering the greater negative CVo–age associations in smokers observed in the categorized analyses, this suggests that chronic smoking of even a small amount per day could be harmful to normal brain aging equivalently to a large dosage.

It is known that alcohol consumption has a U-shaped relationship with the risk of dementia, cardiovascular disease (Ruitenberg et al. 2002; Mukamal et al. 2003; Luchsinger et al.

differences. Fitted age trajectories for Val/Val (solid lines), Val/Met (dashed lines), and Met/Met genotypes (circle, solid lines) are depicted for vertices with maximum *F*-statistic in clusters. (*C*) Associations between COMT Val158Met and age-related CTh differences. Fitted age trajectories for Val/Val (solid lines), Val/Met (dashed lines), and Met/Met genotypes (circle, solid lines) are depicted for vertices with maximum *F*-statistics in clusters. (*D*) Associations of CASS4 rs7274581 (preventive for AD) and age-related CSA differences. Fitted age trajectories for T/T (solid lines), C/T (dashed lines), and C/C genotypes (circle, solid lines) are depicted for vertices with maximum *F*-statistics in clusters. (*E*) Associations between CD2AP rs10948363 (risk for AD) and age-related CSA differences. Fitted age trajectories for A/A (solid lines), A/G (dashed lines), and G/G genotypes (circle, solid lines) are depicted for vertices with maximum *F*-statistics in clusters.

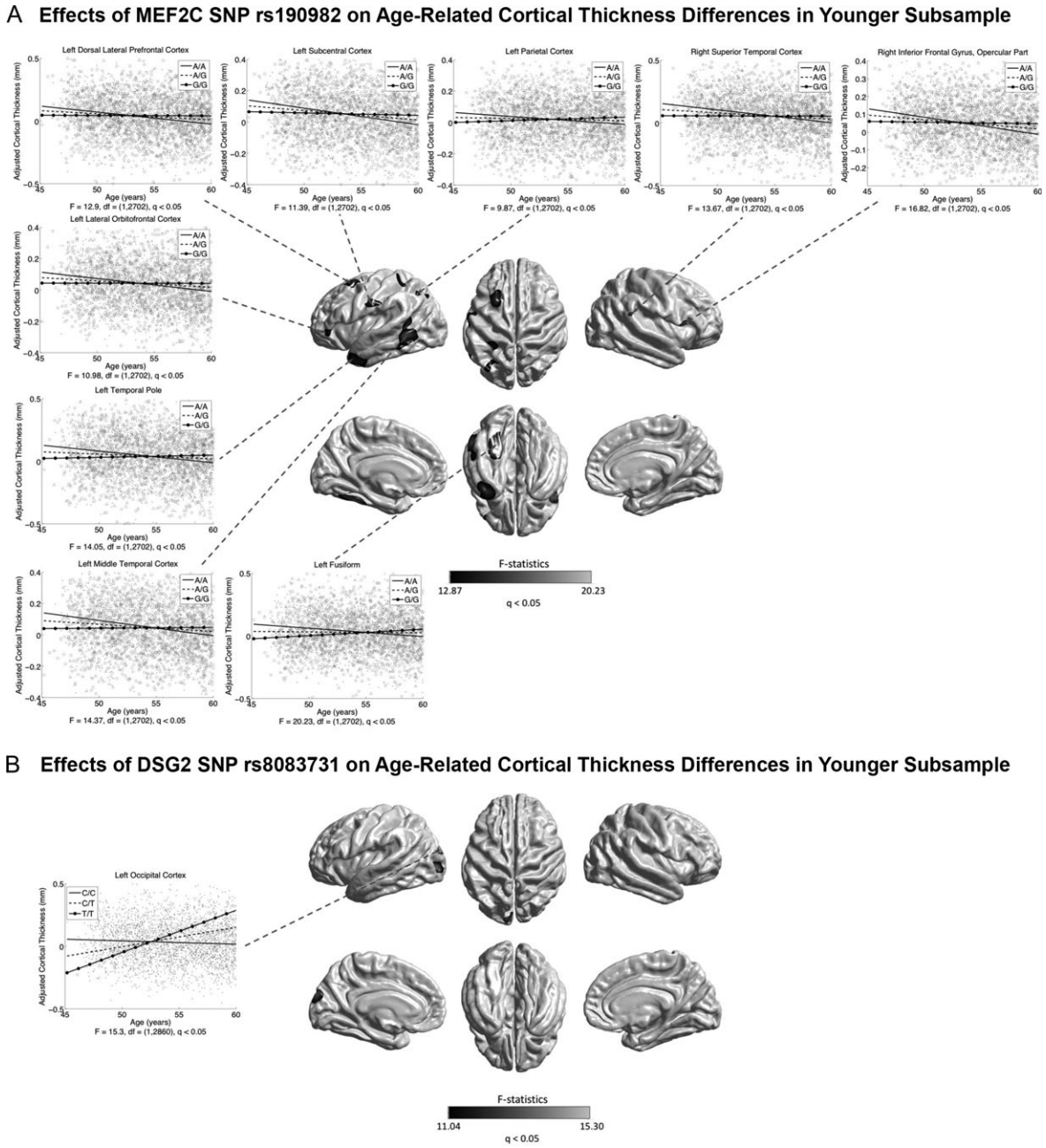

Figure 11. Associations between genetic variants and age-related cortical morphological differences in the younger subsample (≤60 years). Grayscale bar represents *F*-statistics. Areas in black-lightgray represent patterns at the exploratory level of $q < 0.05$. (*A*) Associations between MEF2C rs190982 (preventive for AD) and age-related CTh differences. Fitted age trajectories for A/A (solid lines), A/G (dashed lines), and G/G (circle, solid lines) genotypes are depicted for vertices with maximum *F*-statistics in clusters (*x*-axis = age (years), *y*-axis = CTh adjusted for sex and intracranial volume). (*B*) Associations between DSG2 rs8083731 (preventive for AD) and age-related CTh differences. Fitted age trajectories for C/C (solid lines), C/T (dashed lines), and T/T genotypes (circle solid lines) are depicted for the vertex with maximum *F*-statistic in the cluster.

2004; Bell et al. 2017), and cognitive functions (Mukamal et al. 2003; Stampfer et al. 2005; Piumatti et al. 2018), that is, compared with abstinence, light-to-moderate alcohol consumption is protective, whereas heavy consumption is harmful. Using the SBM framework, we detected widespread patterns of such U-shaped association of alcohol consumption with CTh and CVo (Supplementary Fig. S11). This is especially consistent with the recently reported U-shaped relationship of alcohol consumption with the performance in the reaction time task in the UK Biobank cohort (Piumatti et al. 2018). We further found that, compared with abstinence, alcohol consumption of >30 drinks/week was related to an increased negative cortical morphology–age association in multiple brain regions (at the exploratory level of $q < 0.05$) (Fig. 8). The patterns in the left parahippocampus and the right SFG were also observed in individuals consuming 14–21 and 21–30 drinks/week, respectively (Supplementary Fig. S12). These findings evidence that heavy alcohol use may be related to accelerated cortical decline in normal aging. Trends of reduced negative cortical morphology–age associations (uncorrected $P < 0.05$) relative to abstainers

Table 3 Loadings of the first 10 PCs produced by the group-sparse block PCA

Variables	PC1	PC2	PC3	PC4	PC5	PC6	PC7	PC8	PC9	PC10
Education										
College degree	−0.11	0.47	0.013	−0.029	0.47	−0.12		0.0026		−0.16
No college degree	0.11	−0.47	−0.013	0.029	−0.47	0.12		−0.0026		0.16
Fluid intelligence Score		0.32		−0.017	0.074	0.25	−0.014	0.035	−0.015	0.93
Prospective memory:										
Completed on the first attempt		0.42	0.10	−0.18	0.51	−0.076		0.00053		−0.081
Not completed on the first attempt		−0.42	−0.10	0.18	−0.51	0.076		−0.00053		0.081
Visual memory		−0.081				−0.75	0.080	−0.51	0.25	0.24
Reaction time		−0.13				−0.55	0.054	0.70	−0.42	0.11
Smoking status										
Current	0.14		−0.010	−0.032	−0.026	0.13	0.94			−0.0063
Never	−0.56		0.048	0.13	0.070	0.0089	−0.022			0.0051
Previous	0.52		−0.045	−0.12	−0.062	−0.058	−0.34			−0.0028
Pack-years of Smoking	0.54		−0.044	−0.12	-0.056		0.039			
Alcohol drinker Status										
Current	0.15	0.17	−0.31	0.54	−0.088	−0.018				−0.024
Never	−0.15	−0.17	0.31	−0.54	0.088	0.018				0.024
Alcohol consumption	0.20	0.14	−0.16	0.22				−0.014		
Insomnia:										
Control	−0.026		0.59	−0.35				−0.079	−0.15	
Frequent symptom	0.026		−0.59	0.35				0.079	0.15	
Sleep duration			0.24	−0.12		−0.034		0.49	0.85	
Variance (%)	17.96	14.29	12.58	12.16	10.55	6.67	6.21	5.26	5.13	4.46
Cumulative variance (%)	17.96	32.25	44.83	57.00	67.54	74.22	80.42	85.69	90.81	95.27

Note: Empty cells have zero loadings.

were observed in the ACC, MCC, MTC, SMG, and insula (inconsistently between CTh, CVo, and CSA) in individuals consuming 1–21 drinks/week, which were not seen in individuals consuming >21 drinks/week (Supplementary Figs S16–S18). With caution, this might imply a potential protective effect of light-to-moderate drinking on age-related cortical decline in the specific regions.

Sleep disruption has been suggested as a novel contributing factor to age-related cognitive decline in elderly (Mander et al. 2013; Lo et al. 2014). This study showed that the relatively stable negative CVo–age associations in normal sleepers was disrupted into an inverted U-shaped relationship in multiple cortical regions in participants with frequent insomnia symptoms (at the exploratory level of $q < 0.05$) (Fig. 9B). These disruptions were found to be mostly contributed by CSA (Fig. 9C) rather by CTh, except in the left LING (Fig. 9A). Central nervous system hyperarousal represents a major pathophysiologic pathway in the development and maintenance of insomnia (Riemann et al. 2010; Zhao et al. 2015). Such hyperarousal hypothesis might account for the insomnia-related increase or preservation of cortical structures in middle and early old ages. While, the increased negative cortical morphology–age associations in late old ages may reflect an expression of the cumulative adverse influence of chronic insomnia in earlier life. Our findings may provide a neuroanatomical basis for the insomnia-related cognitive impairments observed in a recent UK Biobank cognitive study (Kyle et al. 2017).

Genetic Effects are More Pronounced in Late Life

The current genetic association analysis was focused on APOE, BDNF, COMT, KOLTHO, and 21 AD GWAS loci. The APOE, BDNF, and COMT genes have been more frequently associated with individual differences in age-sensitive cognitive domains than other genes (Raz et al. 2009). The longevity gene *KLOTHO* is a leading aging suppressor and has been related to enhanced cognition and greater CVo in healthy elderly (Dubal et al. 2014; Yokoyama et al. 2015). The 21 AD loci, in addition to APOE, were identified by the largest GWAS in AD to date (Lambert et al. 2013), many of them have been implicated in brain metabolism and neurodegeneration (Stage et al. 2016). Nevertheless, the influences of these genetic variants on age-related cortical differences remain unclear. Using the whole sample, we found only a regional effect of the *BDNF* gene for CSA (at the exploratory level of $q < 0.05$) (Supplementary Fig. S13), while more distributed genetic associations were detected in the subsample of older participants (>60 years) (Fig. 10). For example, the APOE ε4 allele was associated with greater negative CTh–age associations in AD-prone areas (mTC and PCC) in the older subsample (at the exploratory level of $q < 0.05$) rather in the younger ones (Fig. 10A), consistently with previous findings of more pronounced APOE associations with cognitive declines at older ages (Schiepers et al. 2012; Davies et al. 2015; Marioni et al. 2016). Such phenomenon may be related to the age-related gene expression change in the brain (Lu et al. 2004; Glass et al. 2013). The age-related gene expression change may also account for the contrary directions of the BDNF Val66Met effects reported in young and old samples, that is, Met allele is vulnerable to brain atrophy and cognitive impairment in early life (Egan et al. 2003; Pezawas et al. 2004), whereas Val allele is vulnerable to cognitive declines (Harris et al. 2006) and AD (Ventriglia et al. 2002) in late life. In line with this, we found, in specific brain regions, BDNF Met allele was associated with smaller CVo and CSA at ages younger than around 65 years, while Val allele was associated with regional structural loss at older ages (Fig. 10B and Supplementary Fig. S13). This theory may also apply to the inversed COMT Val158Met effects on CTh in younger and older groups observed here (Fig. 10C) and in

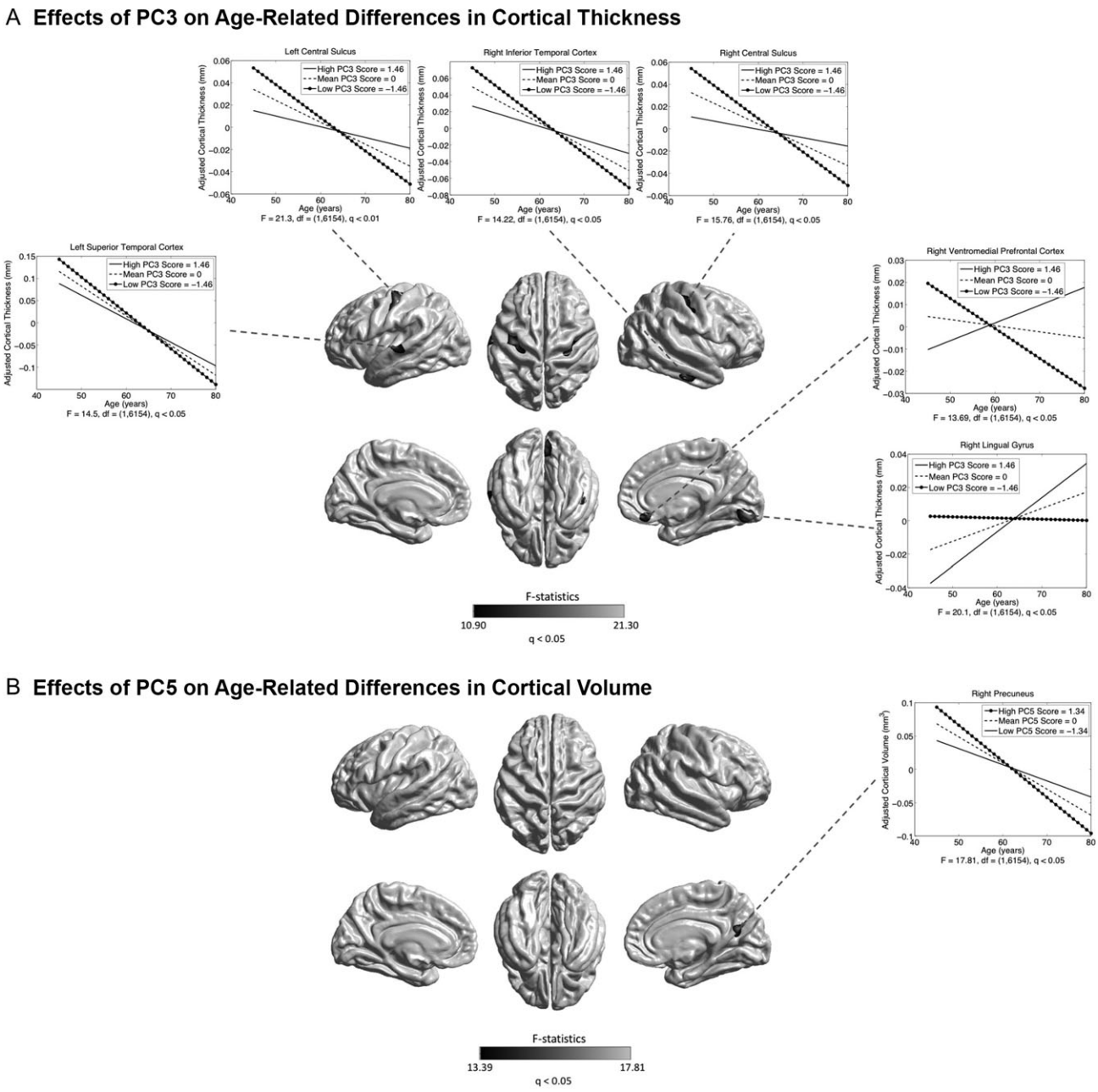

Figure 12. Associations between the third principal component (PC3) and age-related CTh differences (*A*) and between the fifth principal component (PC5) and age-related CVo differences (*B*). Grayscale bar represents *F*-statistics. Areas in black-lightgray represent associations at the exploratory level of $q < 0.05$. Fitted age trajectories for mean PC score (dashed lines), high PC score [mean(PC score) + SD(PC score)] (solid lines), and low PC score [mean(PC score) − SD(PC score)] (circle, solid lines) are depicted for vertices with maximum *F*-statistics in clusters (*x*-axis = age (years), *y*-axis = cortical morphometric measure adjusted for sex and intracranial volume).

previous studies (Lee and Qiu 2016). In the older subsample, 2 AD GWAS loci, CD2AP (rs10948363) and CASS4 (rs7274581), were associated with CSA differences over time (at the exploratory level of $q < 0.05$). The CD2AP is a leading genetic risk factor for AD (Cochran et al. 2015). Here, the minor allele G was linked to increasing negative CSA–age associations after around 65 years (Fig. 10*E*). The exact function of CASS4 is unknown, and the reported associations of this gene with AD are inconsistent. The observed preventive effects of the CASS4 SNP support its preventive role for AD (Lambert et al. 2013) (Fig. 10*D*). In the younger subsample (≤60 years), only 2 preventive AD GWAS loci (Lambert et al. 2013), MEF2C (rs190982) and DSG2 (rs8093731), were found to show preventive effects on negative CTh–age associations (at the exploratory level of $q < 0.05$) (Fig. 11). We could speculate that AD risk factors (e.g., APOE and CD2AP) may pronouncedly function in the brain at older ages (>60 years), whereas preventive factors (e.g., MEF2C and DSG2) may mainly express earlier. It is not surprising that we did not detect any association of the *KLOTHO* gene with age-related cortical differences. It was reported that KLOTHO effects on brain structures seem to be relatively constant across the adulthood (Yokoyama et al. 2015).

Joint Effects of Cognitive, Lifestyle Variables, and Education

The analyses on the first 10 PCs from the group-sparse block PCA showed that PC3 and PC5 were, respectively, associated with age-related CTh differences in the central sulci, the left STC, the right ITC, LING and vmPFC, and age-related CVo differences in the right precuneus (at the exploratory level of $q < 0.05$) (Fig. 12). Compared with the standard PCA, the sparse PCA utilized in this work can offer data dimension reduction with better statistical properties and interpretability, as it produces PCs using only effective variables (Hsu et al. 2014). Consequently, the sparse PCs obtained here were linear combinations of subsets of the studied variables, and the loadings presented the contribution of each variable to the PCs (Sill et al. 2015) (Table 3). Therefore, the result for PC3 reflects a joint effect predominantly determined by sleep factors ($|\text{loading}| > 0.2$), alcohol drinking variables ($|\text{loading}| > 0.15$) and prospective memory performance ($|\text{loading}| = 0.1$), and marginally determined by education and tobacco smoking variables ($|\text{loading}| < 0.1$). Lower PC3 score was correlated with greater negative regional CTh–age associations (Fig. 12A). Since increase in the variables with negative PC loadings and decrease in the variables with positive loadings would contribute to the decrease in PC score, the loadings vector of PC3 (Table 3) suggest that sleep disruption, chronic and larger alcohol consumption and poor prospective memory performance, together with moderate contributions of chronic and larger tobacco consumption and lower education level, would lead to a smaller PC3 score, thus would jointly predict a larger negative CTh–age association in CMC, STC, ITC, LING, and vmPFC. Such finding is largely consistent with the independent tests (Figs 7–9 and Supplementary Figs S3 and S5). Furthermore, PC5 was a combined variable primarily of prospective memory performance and education ($|\text{loading}| > 0.45$), to which fluid intelligence, smoking variables, and alcohol drinker status marginally contributed as well ($|\text{loading}| < 0.1$). The independent analyses only found an association between prospective memory performance and the CTh–age relationship in the right ACC at the exploratory level of $q < 0.05$ (Fig. 6B) and did not detect effect of education on age-related cortical differences. Here, lower PC5 score was correlated with a greater negative CVo–age association in the right precuneus (Fig. 12B). This result revealed that poor prospective memory performance and lower education level, together with peripheral contributions of lower fluid intelligence score, chronic tobacco, and alcohol consumptions, which would result in a reduced PC5 score, could jointly predict a greater negative CVo–age association in the precuneus. These detected joint effects further complement the independent tests for the behavioral and environmental variables and provide a holistic view into the relationships of these factors with age-related cortical morphological differences in middle to older ages.

Limitations

The first limitation in this study is that the cross-sectional nature of the current data prevented us from testing within-individual age-changes in brain morphology. A longitudinal approach with further data is desirable. Second, the age trajectories were constructed using mixed-effect regression models. Although this is a valid method, nonparametric smoothing has been suggested as a better alternative as it may produce a more robust life span trajectory description due to the locality of estimation (Fjell et al. 2010). However, the interactions of various variables of interest with linear and nonlinear age terms assessed here cannot be examined using nonparametric models only except when the interaction involves a sign change. Third, most of the results, except the majority of linear age effects and a part of the quadratic age effects, age trajectory break points and sex differences, only survived the exploratory correction for multiple comparisons across the 327 684 cortical surface vertices at $q < 0.05$, but not the further correction for the multiple whole-brain comparisons. There is a chance that these more lenient results are false positives, nevertheless, the cost of the false positives is just the increased number of whole-brain tests, which is far smaller than the number of vertex-wise tests (219 vs. 327 684) (McDonald 2014). Fourth, latent variables of the behavioral and environmental variables were extracted as linear combinations with PCA modeling. It is conceivable that these linear combinations could not completely explain the joint associations of these factors with age-related cortical differences. There may exist more complex nonlinear combinations, which are desired to be explored in the future, for example, using manifold learning approaches (Lawrence 2012). Fifth, it has been widely reported that the structure of one brain region often changes in a statistically correlated fashion with the changes in some other regions (Alexander-Bloch et al. 2013). Such system-level interregional relationships of the brain have been shown to change with age in development (Zielinski et al. 2010) and aging (Spreng and Turner 2013) or even cross the life span (DuPre and Spreng 2017). It would be meaningful to identify system-level components of age-related brain structural differences or changes using intrinsic network analysis approaches (Beckmann et al. 2005) in the future. Finally, subcortical regions were not included here as this study was based on a cortical surface model. It would also be a meaningful future work to extend the current study to subcortical regions for a more complete understanding of age-differences in brain morphology.

Conclusions

This study quantified localized age-differences in multiple morphometric metrics across the cortex using the large-scale, well-defined UK Biobank brain imaging sample. Allocortex regions (limbic/paralimbic areas), which have simple laminar architecture and arise early in evolution, predominantly showed nonlinear age effects on all structural measures. In contrast, most of 6-layered neocortex areas that evolve later than allocortex only showed a linear age effect. Thus, the complexity of brain structure–age relationships in normal aging may be related to the laminar organization of the cortex and differentials in regional evolutionary ages. This cross-sectional study also revealed age of about 60 as a break point for increasing cortical morphology–age associations in the AD-prone areas. We further reported novel results of diverse associations of the potential modifiers with age-related cortical differences, including the associations of better cognitive functions of fluid intelligence, reaction time and prospective memory with reduced negative cortical morphology–age relationships, the associations of cigarette smoking, excessive alcohol consumption and sleep disruption with greater negative cortical morphology–age relationships, the age-related variations in genetic influences of the APOE, BDNF, COMT genes and several AD GWAS loci, and the joint effects of cognitive, lifestyle variables, and education. In sum, this study provides a population-based characterization of age-related brain structural differences in middle to older ages, and a comprehensive description of how and to what

extent the demographic, cognitive, lifestyle, and genetic factors are associated with the age–brain structure relationships.

Supplementary Material

Supplementary material is available at *Cerebral Cortex* online.

Funding

This work was supported by the Big Data for Discovery Science (BDDS) (NIH Grant No. U54EB020406), the Laboratory of Neuro Imaging Resource (LONIR) (NIH Grant No. P41EB015922), and the Genetic Influences on Human Neuroanatomical Shapes (NIH Grant No. R01MH094343).

Notes

This research was conducted, using the UK Biobank Resource under approved project 25 641. *Conflict of Interests*: All the authors declare no biomedical financial interests or potential conflicts of interest regarding the publication of this paper.

References

Alexander-Bloch A, Giedd JN, Bullmore E. 2013. Imaging structural co-variance between human brain regions. Nat Rev Neurosci. 14:322–336.

Alfaro-Almagro F, Jenkinson M, Bangerter NK, Andersson JLR, Griffanti L, Douaud G, Sotiropoulos SN, Jbabdi S, Hernandez-Fernandez M, Vallee E, et al. 2017. Image processing and quality control for the first 10,000 brain imaging datasets from UK Biobank. Neuroimage. 166:400–424.

Beckmann CF, DeLuca M, Devlin JT, Smith SM. 2005. Investigations into resting-state connectivity using independent component analysis. Philos Trans R Soc Lond B Biol Sci. 360:1001–1013.

Bell S, Daskalopoulou M, Rapsomaniki E, George J, Britton A, Bobak M, Casas JP, Dale CE, Denaxas S, Shah AD, et al. 2017. Association between clinically recorded alcohol consumption and initial presentation of 12 cardiovascular diseases: population based cohort study using linked health records. BMJ. 356:j909.

Burgmans S, van Boxtel MP, Vuurman EF, Smeets F, Gronenschild EH, Uylings HB, Jolles J. 2009. The prevalence of cortical gray matter atrophy may be overestimated in the healthy aging brain. Neuropsychology. 23:541–550.

Cannon R, Lubar J. 2011. Long-term effects of neurofeedback training in anterior cingulate cortex: a short follow-up report. J Neurotherapy. 15:130–150.

Chavent M, Chavent G 2017. Group-sparse block PCA and explained variance. arXiv:170500461.

Chiang MC, Barysheva M, Shattuck DW, Lee AD, Madsen SK, Avedissian C, Klunder AD, Toga AW, McMahon KL, de Zubicaray GI, et al. 2009. Genetics of brain fiber architecture and intellectual performance. J Neurosci. 29:2212–2224.

Choi YY, Shamosh NA, Cho SH, DeYoung CG, Lee MJ, Lee JM, Kim SI, Cho ZH, Kim K, Gray JR, et al. 2008. Multiple bases of human intelligence revealed by cortical thickness and neural activation. J Neurosci. 28:10323–10329.

Cochran JN, Rush T, Buckingham SC, Roberson ED. 2015. The Alzheimer's disease risk factor CD2AP maintains blood-brain barrier integrity. Hum Mol Genet. 24:6667–6674.

Cona G, Scarpazza C, Sartori G, Moscovitch M, Bisiacchi PS. 2015. Neural bases of prospective memory: a meta-analysis and the "Attention to Delayed Intention" (AtoDI) model. Neurosci Biobehav Rev. 52:21–37.

Crivello F, Tzourio-Mazoyer N, Tzourio C, Mazoyer B. 2014. Longitudinal assessment of global and regional rate of grey matter atrophy in 1,172 healthy older adults: modulation by sex and age. PLoS One. 9:e114478.

Davatzikos C, Xu F, An Y, Fan Y, Resnick SM. 2009. Longitudinal progression of Alzheimer's-like patterns of atrophy in normal older adults: the SPARE-AD index. Brain. 132:2026–2035.

Davies G, Armstrong N, Bis JC, Bressler J, Chouraki V, Giddaluru S, Hofer E, Ibrahim-Verbaas CA, Kirin M, Lahti J, et al. 2015. Genetic contributions to variation in general cognitive function: a meta-analysis of genome-wide association studies in the CHARGE consortium (N = 53949). Mol Psychiatry. 20:183–192.

Dickerson BC, Feczko E, Augustinack JC, Pacheco J, Morris JC, Fischl B, Buckner RL. 2009. Differential effects of aging and Alzheimer's disease on medial temporal lobe cortical thickness and surface area. Neurobiol Aging. 30:432–440.

Dotson VM, Szymkowicz SM, Sozda CN, Kirton JW, Green ML, O'Shea A, McLaren ME, Anton SD, Manini TM, Woods AJ. 2015. Age differences in prefrontal surface area and thickness in middle aged to older adults. Front Aging Neurosci. 7:250.

Dubal DB, Yokoyama JS, Zhu L, Broestl L, Worden K, Wang D, Sturm VE, Kim D, Klein E, Yu GQ, et al. 2014. Life extension factor klotho enhances cognition. Cell Rep. 7:1065–1076.

Dubal DB, Zhu L, Sanchez PE, Worden K, Broestl L, Johnson E, Ho K, Yu GQ, Kim D, Betourne A, et al. 2015. Life extension factor klotho prevents mortality and enhances cognition in hAPP transgenic mice. J Neurosci. 35:2358–2371.

DuPre E, Spreng RN. 2017. Structural covariance networks across the life span, from 6 to 94 years of age. Netw Neurosci. 1:302–323.

Durazzo TC, Insel PS, Weiner MW, Alzheimer Disease Neuroimaging I. 2012. Greater regional brain atrophy rate in healthy elderly subjects with a history of cigarette smoking. Alzheimers Dement. 8:513–519.

Egan MF, Kojima M, Callicott JH, Goldberg TE, Kolachana BS, Bertolino A, Zaitsev E, Gold B, Goldman D, Dean M, et al. 2003. The BDNF val66met polymorphism affects activity-dependent secretion of BDNF and human memory and hippocampal function. Cell. 112:257–269.

Engvig A, Fjell AM, Westlye LT, Moberget T, Sundseth O, Larsen VA, Walhovd KB. 2010. Effects of memory training on cortical thickness in the elderly. Neuroimage. 52:1667–1676.

Fischl B, Dale AM. 2000. Measuring the thickness of the human cerebral cortex from magnetic resonance images. Proc Natl Acad Sci USA. 97:11050–11055.

Fjell AM, Walhovd KB. 2010. Structural brain changes in aging: courses, causes and cognitive consequences. Rev Neurosci. 21:187–221.

Fjell AM, Walhovd KB, Fennema-Notestine C, McEvoy LK, Hagler DJ, Holland D, Brewer JB, Dale AM. 2009. One-year brain atrophy evident in healthy aging. J Neurosci. 29:15223–15231.

Fjell AM, Walhovd KB, Westlye LT, Ostby Y, Tamnes CK, Jernigan TL, Gamst A, Dale AM. 2010. When does brain aging accelerate? Dangers of quadratic fits in cross-sectional studies. Neuroimage. 50:1376–1383.

Fjell AM, Westlye LT, Grydeland H, Amlien I, Espeseth T, Reinvang I, Raz N, Dale AM, Walhovd KB, Alzheimer Disease

Neuroimaging I. 2014. Accelerating cortical thinning: unique to dementia or universal in aging? Cereb Cortex. 24:919–934.
Fowler JS, Volkow ND, Kassed CA, Chang L. 2007. Imaging the addicted human brain. Sci Pract Perspect. 3:4–16.
Ghebranious N, Ivacic L, Mallum J, Dokken C. 2005. Detection of ApoE E2, E3 and E4 alleles using MALDI-TOF mass spectrometry and the homogeneous mass-extend technology. Nucleic Acids Res. 33:e149.
Glass D, Vinuela A, Davies MN, Ramasamy A, Parts L, Knowles D, Brown AA, Hedman AK, Small KS, Buil A, et al. 2013. Gene expression changes with age in skin, adipose tissue, blood and brain. Genome Biol. 14:R75.
Gogtay N, Giedd JN, Lusk L, Hayashi KM, Greenstein D, Vaituzis AC, Nugent TF 3rd, Herman DH, Clasen LS, Toga AW, et al. 2004. Dynamic mapping of human cortical development during childhood through early adulthood. Proc Natl Acad Sci USA. 101:8174–8179.
Gunning-Dixon FM, Brickman AM, Cheng JC, Alexopoulos GS. 2009. Aging of cerebral white matter: a review of MRI findings. Int J Geriatr Psychiatry. 24:109–117.
Gur RE, Gur RC. 2002. Gender differences in aging: cognition, emotions, and neuroimaging studies. Dialogues Clin Neurosci. 4:197–210.
Hagger-Johnson G, Sabia S, Brunner EJ, Shipley M, Bobak M, Marmot M, Kivimaki M, Singh-Manoux A. 2013. Combined impact of smoking and heavy alcohol use on cognitive decline in early old age: Whitehall II prospective cohort study. Br J Psychiatry. 203:120–125.
Harada CN, Natelson Love MC, Triebel KL. 2013. Normal cognitive aging. Clin Geriatr Med. 29:737–752.
Harris SE, Fox H, Wright AF, Hayward C, Starr JM, Whalley LJ, Deary IJ. 2006. The brain-derived neurotrophic factor Val66Met polymorphism is associated with age-related change in reasoning skills. Mol Psychiatry. 11:505–513.
Hogstrom LJ, Westlye LT, Walhovd KB, Fjell AM. 2013. The structure of the cerebral cortex across adult life: age-related patterns of surface area, thickness, and gyrification. Cereb Cortex. 23:2521–2530.
Holland J, Bandelow S, Hogervorst E. 2011. Testosterone levels and cognition in elderly men: a review. Maturitas. 69: 322–337.
Hsu YL, Huang PY, Chen DT. 2014. Sparse principal component analysis in cancer research. Transl Cancer Res. 3:182–190.
Jack CR Jr., Knopman DS, Jagust WJ, Shaw LM, Aisen PS, Weiner MW, Petersen RC, Trojanowski JQ. 2010. Hypothetical model of dynamic biomarkers of the Alzheimer's pathological cascade. Lancet Neurol. 9:119–128.
Journée M, Nesterov Y, Richtárik P, Sepulchre R. 2010. Generalized power method for sparse principal component analysis. J Mach Learn Res. 11:517–553.
Karama S, Bastin ME, Murray C, Royle NA, Penke L, Munoz Maniega S, Gow AJ, Corley J, Valdes Hernandez Mdel C, Lewis JD, et al. 2014. Childhood cognitive ability accounts for associations between cognitive ability and brain cortical thickness in old age. Mol Psychiatry. 19:555–559.
Karama S, Ducharme S, Corley J, Chouinard-Decorte F, Starr JM, Wardlaw JM, Bastin ME, Deary IJ. 2015. Cigarette smoking and thinning of the brain's cortex. Mol Psychiatry. 20: 778–785.
Kassem MS, Lagopoulos J, Stait-Gardner T, Price WS, Chohan TW, Arnold JC, Hatton SN, Bennett MR. 2013. Stress-induced grey matter loss determined by MRI is primarily due to loss of dendrites and their synapses. Mol Neurobiol. 47:645–661.
Kaup AR, Mirzakhanian H, Jeste DV, Eyler LT. 2011. A review of the brain structure correlates of successful cognitive aging. J Neuropsychiatry Clin Neurosci. 23:6–15.
Kennedy KM, Raz N. 2015. Normal aging of the brain. In: Toga A, editor. Brain mapping: an encyclopedia reference. London/San Diego/Waltham/Oxford: Elsevier. p. 603–617.
Kyle SD, Sexton CE, Feige B, Luik AI, Lane J, Saxena R, Anderson SG, Bechtold DA, Dixon W, Little MA, et al. 2017. Sleep and cognitive performance: cross-sectional associations in the UK Biobank. Sleep Med. 38:85–91.
Lambert JC, Ibrahim-Verbaas CA, Harold D, Naj AC, Sims R, Bellenguez C, DeStafano AL, Bis JC, Beecham GW, Grenier-Boley B, et al. 2013. Meta-analysis of 74,046 individuals identifies 11 new susceptibility loci for Alzheimer's disease. Nat Genet. 45:1452–1458.
Lawrence ND. 2012. A unifying probabilistic perspective for spectral dimensionality reduction: insights and new models. J Mach Learn Res. 13:1609–1638.
Lee A, Qiu A. 2016. Modulative effects of COMT haplotype on age-related associations with brain morphology. Hum Brain Mapp. 37:2068–2082.
Lemaitre H, Goldman AL, Sambataro F, Verchinski BA, Meyer-Lindenberg A, Weinberger DR, Mattay VS. 2012. Normal age-related brain morphometric changes: nonuniformity across cortical thickness, surface area and gray matter volume? Neurobiol Aging. 33:617 e611–617 e619.
Lenroot RK, Gogtay N, Greenstein DK, Wells EM, Wallace GL, Clasen LS, Blumenthal JD, Lerch J, Zijdenbos AP, Evans AC, et al. 2007. Sexual dimorphism of brain developmental trajectories during childhood and adolescence. Neuroimage. 36:1065–1073.
Leong RLF, Lo JC, Sim SKY, Zheng H, Tandi J, Zhou J, Chee MWL. 2017. Longitudinal brain structure and cognitive changes over 8 years in an East Asian cohort. Neuroimage. 147: 852–860.
Lo JC, Groeger JA, Cheng GH, Dijk DJ, Chee MW. 2016. Self-reported sleep duration and cognitive performance in older adults: a systematic review and meta-analysis. Sleep Med. 17:87–98.
Lo JC, Loh KK, Zheng H, Sim SK, Chee MW. 2014. Sleep duration and age-related changes in brain structure and cognitive performance. Sleep. 37:1171–1178.
Lu T, Pan Y, Kao SY, Li C, Kohane I, Chan J, Yankner BA. 2004. Gene regulation and DNA damage in the ageing human brain. Nature. 429:883–891.
Luchsinger JA, Tang MX, Siddiqui M, Shea S, Mayeux R. 2004. Alcohol intake and risk of dementia. J Am Geriatr Soc. 52: 540–546.
Luders E, Narr KL, Thompson PM, Toga AW. 2009. Neuroanatomical correlates of intelligence. Intelligence. 37:156–163.
Lyall DM, Cullen B, Allerhand M, Smith DJ, Mackay D, Evans J, Anderson J, Fawns-Ritchie C, McIntosh AM, Deary IJ, et al. 2016. Cognitive test scores in UK Biobank: data reduction in 480,416 participants and longitudinal stability in 20,346 participants. PLoS One. 11:e0154222.
Malpetti M, Ballarini T, Presotto L, Garibotto V, Tettamanti M, Perani D, Alzheimer's Disease Neuroimaging Initiative d, Network for E, Standardization of Dementia Diagnosis d. 2017. Gender differences in healthy aging and Alzheimer's dementia: a (18) F-FDG-PET study of brain and cognitive reserve. Hum Brain Mapp. 38:4212–4227.
Mander BA, Rao V, Lu B, Saletin JM, Lindquist JR, Ancoli-Israel S, Jagust W, Walker MP. 2013. Prefrontal atrophy, disrupted

NREM slow waves and impaired hippocampal-dependent memory in aging. Nat Neurosci. 16:357–364.

Marioni RE, Campbell A, Scotland G, Hayward C, Porteous DJ, Deary IJ. 2016. Differential effects of the APOE e4 allele on different domains of cognitive ability across the life-course. Eur J Hum Genet. 24:919–923.

McDonald JH. 2014. Handbook of biological statistics. 3rd ed. Baltimore, Maryland: Sparky House.

Menary K, Collins PF, Porter JN, Muetzel R, Olson EA, Kumar V, Steinbach M, Lim KO, Luciana M. 2013. Associations between cortical thickness and general intelligence in children, adolescents and young adults. Intelligence. 41: 597–606.

Miller KL, Alfaro-Almagro F, Bangerter NK, Thomas DL, Yacoub E, Xu J, Bartsch AJ, Jbabdi S, Sotiropoulos SN, Andersson JL, et al. 2016. Multimodal population brain imaging in the UK Biobank prospective epidemiological study. Nat Neurosci. 19:1523–1536.

Muggeo VM. 2003. Estimating regression models with unknown break-points. Stat Med. 22:3055–3071.

Muggeo VM. 2008. Segmented: an R package to fit regression models with broken-line relationships. R News. 8:20–25.

Muggeo VM. 2016. Testing with a nuisance parameter present only under the alternative: a score-based approach with application to segmented modelling. J Stat Comput Simul. 86:3059–3067.

Mukamal KJ, Kuller LH, Fitzpatrick AL, Longstreth WT Jr., Mittleman MA, Siscovick DS. 2003. Prospective study of alcohol consumption and risk of dementia in older adults. JAMA. 289:1405–1413.

Murre JM, Sturdy DP. 1995. The connectivity of the brain: multi-level quantitative analysis. Biol Cybern. 73:529–545.

Naito E, Kinomura S, Geyer S, Kawashima R, Roland PE, Zilles K. 2000. Fast reaction to different sensory modalities activates common fields in the motor areas, but the anterior cingulate cortex is involved in the speed of reaction. J Neurophysiol. 83:1701–1709.

Panizzon MS, Fennema-Notestine C, Eyler LT, Jernigan TL, Prom-Wormley E, Neale M, Jacobson K, Lyons MJ, Grant MD, Franz CE, et al. 2009. Distinct genetic influences on cortical surface area and cortical thickness. Cereb Cortex. 19:2728–2735.

Peper JS, Brouwer RM, Boomsma DI, Kahn RS, Hulshoff Pol HE. 2007. Genetic influences on human brain structure: a review of brain imaging studies in twins. Hum Brain Mapp. 28: 464–473.

Persson J, Pudas S, Lind J, Kauppi K, Nilsson LG, Nyberg L. 2012. Longitudinal structure-function correlates in elderly reveal MTL dysfunction with cognitive decline. Cereb Cortex. 22: 2297–2304.

Pezawas L, Verchinski BA, Mattay VS, Callicott JH, Kolachana BS, Straub RE, Egan MF, Meyer-Lindenberg A, Weinberger DR. 2004. The brain-derived neurotrophic factor val66met polymorphism and variation in human cortical morphology. J Neurosci. 24:10099–10102.

Pfefferbaum A, Rohlfing T, Rosenbloom MJ, Chu W, Colrain IM, Sullivan EV. 2013. Variation in longitudinal trajectories of regional brain volumes of healthy men and women (ages 10 to 85 years) measured with atlas-based parcellation of MRI. Neuroimage. 65:176–193.

Piumatti G, Moore SC, Berridge DM, Sarkar C, Gallacher J. 2018. The relationship between alcohol use and long-term cognitive decline in middle and late life: a longitudinal analysis using UK Biobank. J Public Health (Oxf). 40:313–314.

Pontious A, Kowalczyk T, Englund C, Hevner RF. 2008. Role of intermediate progenitor cells in cerebral cortex development. Dev Neurosci. 30:24–32.

Posthuma D, De Geus EJ, Baare WF, Hulshoff Pol HE, Kahn RS, Boomsma DI. 2002. The association between brain volume and intelligence is of genetic origin. Nat Neurosci. 5:83–84.

Rakic P. 1988. Specification of cerebral cortical areas. Science. 241:170–176.

Raz N, Ghisletta P, Rodrigue KM, Kennedy KM, Lindenberger U. 2010. Trajectories of brain aging in middle-aged and older adults: regional and individual differences. Neuroimage. 51: 501–511.

Raz N, Gunning FM, Head D, Dupuis JH, McQuain J, Briggs SD, Loken WJ, Thornton AE, Acker JD. 1997. Selective aging of the human cerebral cortex observed in vivo: differential vulnerability of the prefrontal gray matter. Cereb Cortex. 7: 268–282.

Raz N, Lindenberger U, Rodrigue KM, Kennedy KM, Head D, Williamson A, Dahle C, Gerstorf D, Acker JD. 2005. Regional brain changes in aging healthy adults: general trends, individual differences and modifiers. Cereb Cortex. 15: 1676–1689.

Raz N, Rodrigue KM, Kennedy KM, Land S. 2009. Genetic and vascular modifiers of age-sensitive cognitive skills: effects of COMT, BDNF, ApoE, and hypertension. Neuropsychology. 23: 105–116.

Reuter-Lorenz PA, Park DC. 2010. Human neuroscience and the aging mind: a new look at old problems. J Gerontol B Psychol Sci Soc Sci. 65:405–415.

Riemann D, Spiegelhalder K, Feige B, Voderholzer U, Berger M, Perlis M, Nissen C. 2010. The hyperarousal model of insomnia: a review of the concept and its evidence. Sleep Med Rev. 14:19–31.

Righart R, Duering M, Gonik M, Jouvent E, Reyes S, Herve D, Chabriat H, Dichgans M. 2013. Impact of regional cortical and subcortical changes on processing speed in cerebral small vessel disease. Neuroimage Clin. 2:854–861.

Roe M, Pinchen H, Church S, Finglas P. 2015. McCance and Widdowson's the composition of foods seventh summary edition and updated composition of foods integrated dataset. Nutr Bull. 40:36–39.

Ruitenberg A, van Swieten JC, Witteman JC, Mehta KM, van Duijn CM, Hofman A, Breteler MM. 2002. Alcohol consumption and risk of dementia: the Rotterdam Study. Lancet. 359: 281–286.

Salat DH, Buckner RL, Snyder AZ, Greve DN, Desikan RS, Busa E, Morris JC, Dale AM, Fischl B. 2004. Thinning of the cerebral cortex in aging. Cereb Cortex. 14:721–730.

Salat DH, Greve DN, Pacheco JL, Quinn BT, Helmer KG, Buckner RL, Fischl B. 2009. Regional white matter volume differences in nondemented aging and Alzheimer's disease. Neuroimage. 44:1247–1258.

Schiepers OJ, Harris SE, Gow AJ, Pattie A, Brett CE, Starr JM, Deary IJ. 2012. APOE E4 status predicts age-related cognitive decline in the ninth decade: longitudinal follow-up of the Lothian Birth Cohort 1921. Mol Psychiatry. 17:315–324.

Shaw P, Kabani NJ, Lerch JP, Eckstrand K, Lenroot R, Gogtay N, Greenstein D, Clasen L, Evans A, Rapoport JL, et al. 2008. Neurodevelopmental trajectories of the human cerebral cortex. J Neurosci. 28:3586–3594.

Shen H, Huang JZ. 2008. Sparse principal component analysis via regularized low rank matrix approximation. J Multivariate Anal. 99:1015–1034.

Sill M, Saadati M, Benner A. 2015. Applying stability selection to consistently estimate sparse principal components in high-dimensional molecular data. Bioinformatics. 31:2683–2690.

Spreng RN, Turner GR. 2013. Structural covariance of the default network in healthy and pathological aging. J Neurosci. 33: 15226–15234.

Stage E, Duran T, Risacher SL, Goukasian N, Do TM, West JD, Wilhalme H, Nho K, Phillips M, Elashoff D, et al. 2016. The effect of the top 20 Alzheimer disease risk genes on gray-matter density and FDG PET brain metabolism. Alzheimers Dement (Amst). 5:53–66.

Stampfer MJ, Kang JH, Chen J, Cherry R, Grodstein F. 2005. Effects of moderate alcohol consumption on cognitive function in women. N Engl J Med. 352:245–253.

Storsve AB, Fjell AM, Tamnes CK, Westlye LT, Overbye K, Aasland HW, Walhovd KB. 2014. Differential longitudinal changes in cortical thickness, surface area and volume across the adult life span: regions of accelerating and decelerating change. J Neurosci. 34:8488–8498.

Striedter GF. 2006. Precis of principles of brain evolution. Behav Brain Sci. 29:1–12. discussion 1236.

Takahashi R, Ishii K, Kakigi T, Yokoyama K. 2011. Gender and age differences in normal adult human brain: voxel-based morphometric study. Hum Brain Mapp. 32:1050–1058.

Terribilli D, Schaufelberger MS, Duran FL, Zanetti MV, Curiati PK, Menezes PR, Scazufca M, Amaro E Jr., Leite CC, Busatto GF. 2011. Age-related gray matter volume changes in the brain during non-elderly adulthood. Neurobiol Aging. 32:354–368.

Thambisetty M, Wan J, Carass A, An Y, Prince JL, Resnick SM. 2010. Longitudinal changes in cortical thickness associated with normal aging. Neuroimage. 52:1215–1223.

Thompson P, Cannon TD, Toga AW. 2002. Mapping genetic influences on human brain structure. Ann Med. 34:523–536.

Toga AW, Thompson PM. 2005. Genetics of brain structure and intelligence. Annu Rev Neurosci. 28:1–23.

Topiwala A, Allan CL, Valkanova V, Zsoldos E, Filippini N, Sexton C, Mahmood A, Fooks P, Singh-Manoux A, Mackay CE, et al. 2017. Moderate alcohol consumption as risk factor for adverse brain outcomes and cognitive decline: longitudinal cohort study. BMJ. 357:j2353.

Ventriglia M, Bocchio Chiavetto L, Benussi L, Binetti G, Zanetti O, Riva MA, Gennarelli M. 2002. Association between the BDNF 196 A/G polymorphism and sporadic Alzheimer's disease. Mol Psychiatry. 7:136–137.

Watson NF, Badr MS, Belenky G, Bliwise DL, Buxton OM, Buysse D, Dinges DF, Gangwisch J, Grandner MA, Kushida C, et al. 2015. Recommended amount of sleep for a healthy adult: a joint consensus statement of the American Academy of Sleep Medicine and Sleep Research Society. Sleep. 38:843–844.

Westlye LT, Walhovd KB, Dale AM, Bjornerud A, Due-Tonnessen P, Engvig A, Grydeland H, Tamnes CK, Ostby Y, Fjell AM. 2010. Life-span changes of the human brain white matter: diffusion tensor imaging (DTI) and volumetry. Cereb Cortex. 20:2055–2068.

White T, Su S, Schmidt M, Kao CY, Sapiro G. 2010. The development of gyrification in childhood and adolescence. Brain Cogn. 72:36–45.

Winkler AM, Kochunov P, Blangero J, Almasy L, Zilles K, Fox PT, Duggirala R, Glahn DC. 2010. Cortical thickness or grey matter volume? The importance of selecting the phenotype for imaging genetics studies. Neuroimage. 53:1135–1146.

Yang Z, Wen W, Jiang J, Crawford JD, Reppermund S, Levitan C, Slavin MJ, Kochan NA, Richmond RL, Brodaty H, et al. 2016. Age-associated differences on structural brain MRI in non-demented individuals from 71 to 103 years. Neurobiol Aging. 40:86–97.

Yokoyama JS, Sturm VE, Bonham LW, Klein E, Arfanakis K, Yu L, Coppola G, Kramer JH, Bennett DA, Miller BL, et al. 2015. Variation in longevity gene KLOTHO is associated with greater cortical volumes. Ann Clin Transl Neurol. 2:215–230.

Zhao L, Boucher M, Rosa-Neto P, Evans AC. 2013. Impact of scale space search on age- and gender-related changes in MRI-based cortical morphometry. Hum Brain Mapp. 34:2113–2128.

Zhao L, Wang E, Zhang X, Karama S, Khundrakpam B, Zhang H, Guan M, Wang M, Cheng J, Shi D, et al. 2015. Cortical structural connectivity alterations in primary insomnia: insights from MRI-based morphometric correlation analysis. Biomed Res Int. 2015:817595.

Ziegler G, Dahnke R, Jancke L, Yotter RA, May A, Gaser C. 2012. Brain structural trajectories over the adult lifespan. Hum Brain Mapp. 33:2377–2389.

Zielinski BA, Gennatas ED, Zhou J, Seeley WW. 2010. Network-level structural covariance in the developing brain. Proc Natl Acad Sci USA. 107:18191–18196.

Zilles K, Palomero-Gallagher N, Amunts K. 2015. Cytoarchitecture and maps of the cerebral cortex. In: Toga A, editor. Brain mapping an encyclopedic reference. London/San Diego/Waltham/Oxford: Elsevier. p. 115–135.